EVALUATION OF SURFACTANT-MODIFIED ZEOLITE FOR CONTROL OF *CRYPTOSPORIDIUM* AND *GIARDIA* SPECIES IN DRINKING WATER

by

Charlotte Maria Salazar

Submitted in Partial Fulfillment
of Requirements for the

Master of Science in Hydrology

New Mexico Institute of Mining and Technology
Department of Earth and Environmental Science

Socorro, New Mexico

May 2004

ABSTRACT

Gastrointestinal infection due to biological contamination of drinking water supplies is a major health issue worldwide. Naturally occurring and inexpensive modified materials such as surfactant-modified zeolites (SMZ) have net positive surface charge, which may prove useful for adsorption of pathogens such as *Cryptosporidium parvum* and *Giardia intestinales (lamblia)*. SMZ is engineered by modifying the concentration of surfactant hexadecyltrimethylammonium (HDTMA) on the surface of zeolite media. Two different SMZ formulations (cationic SMZ and hydrophobic SMZ) were engineered to develop the most effective media for pathogen removal from drinking water.

In the laboratory, batch experiments of SMZ, raw zeolite, and sand were conducted to determine pathogen sorption to the media. Then, vertical columns packed with SMZ or zeolite material were used to evaluate pathogen transport. Tritium tracer tests were used to determine hydraulic properties of the materials. Synthetic microspheres were used as surrogates for the pathogens, which simulated the size and charge characteristics of *Cryptosporidium* and *Giardia*. The effectiveness of the various SMZ formulations was evaluated by comparing linear distribution coefficients of the batch experiments and removal efficiencies of the microsphere breakthrough curves (BTCs) obtained from the column experiments.

Surfactant-modified zeolite removed *Cryptosporidium* and *Giardia* surrogates from solution in the batch experiments with K_d values 10 to 20 times higher than those for zeolite or sand. This may be due to electrostatic and or hydrophobic interactions between the positively charged SMZ formulations and the negatively charged microspheres. However, column experiments did not show similar results. Based on column studies, all materials had relatively the same removal efficiencies in the range of 79.7(±1.6) to 82.3(±0.8)% for the *Cryptosporidium* surrogates and 99.1(±0.4) to 99.3(±0.1)% for the *Giardia* surrogates, which indicates that physical filtration or gravitational settling were the dominant mechanisms of removal rather than electrostatic or hydrophobic interactions.

ACKNOWLEDGEMENTS

This project was funded by the Waste-management Education and Research Consortium (WERC) and the Alliance for Graduate Education and the Professorate (AGEP). I would like to thank my advisor at New Mexico Tech, Dr. Robert Bowman, and joint project workers from the University of Texas in El Paso, Dr. Dirk Schulze-Makuch and Tanya Lehner. I would like to thank Pat Freeman, President of the St. Cloud mine for donating zeolite. I would like to thank the faculty, staff, and students that assisted with this project: Dr. Buckley, Dr. Cal, Dr. Huang, Dr. Phillips, Dr. Rogelj, Dr. Smoake, Elizabeth Bryant, Jim Elliot, Tom Dotson, Tianguang Fan, Aaron Jenkins, and Talon Newton. Most importantly I would like to thank my supportive husband and my patient 2-year-old son, whom forced me to get out of the lab at least once a day and take a walk to the park.

TABLE OF CONTENTS

LIST OF FIGURES

LIST OF TABLES

Page

LIST OF APPENDICES FIGURES

LIST OF APPENDICES TABLES

INTRODUCTION

This document is the result of a thesis project, which contains a journal article and supporting appendices. The thesis project partially fulfills the requirements for the Degree of Master of Science in Hydrology at the New Mexico Institute of Mining and Technology. The study evaluated the use of surfactant-modified zeolite for treatment of *Cryptosporidium* and *Giardia* in drinking water. The objectives of the study were to develop two surfactant-modified zeolite formulations, evaluate their surface properties, and evaluate their effectiveness of adsorbing pathogens from drinking water.

The following manuscript, entitled "Evaluation of Surfactant-Modified Zeolites for Control of *Cryptosporidium* and *Giardia* Species in Drinking Water," was prepared for submission to a scientific journal, and follows the editorial guidelines set by the American Society of Civil Engineers. The article presents the results of laboratory batch and column experiments, which accomplished the project objectives.

The appendices contain information on preliminary column experiments, detailed descriptions of experimental procedures, and the results from the experiments that were conducted.

EVALUATION OF SURFACTANT-MODIFIED ZEOLITES FOR CONTROL OF *CRYPTOSPORIDIUM* AND *GIARDIA* SPECIES IN DRINKING WATER

Charlotte M. Salazar[1], Robert S. Bowman[2], and Dirk Schultze-Makuch[3]

ABSTRACT

Gastrointestinal infection due to biological contamination of drinking water supplies is a major health issue worldwide. Naturally occurring and inexpensive modified materials such as surfactant-modified zeolites (SMZ) have net positive surface charge, which may prove useful for adsorption of pathogens such as *Cryptosporidium parvum* and *Giardia intestinales (lamblia)*. SMZ is engineered by modifying the concentration of surfactant hexadecyltrimethylammonium (HDTMA) on the surface of zeolite media. Two different SMZ formulations (cationic SMZ and hydrophobic SMZ) were engineered to develop the most effective media for pathogen removal from drinking water.

In the laboratory, batch experiments of SMZ, raw zeolite, and sand were conducted to determine pathogen sorption to the media. Then, vertical columns packed with SMZ or zeolite material were used to evaluate pathogen transport. Tritium tracer tests were used to determine hydraulic properties of the materials. Synthetic microspheres

[1] Department of Earth and Environmental Science, New Mexico Tech, Socorro, NM 87801.
[2] Department of Earth and Environmental Science, New Mexico Tech, Socorro, NM 87801(corresponding author). E-mail: bowman@nmt.edu
[3] Department of Geological Science, University of Texas at El Paso, TX, 79968.

were used as surrogates for the pathogens, which simulated the size and charge characteristics of *Cryptosporidium* and *Giardia*. The effectiveness of the various SMZ formulations was evaluated by comparing linear distribution coefficients of the batch experiments and removal efficiencies of the microsphere breakthrough curves (BTCs) obtained from the column experiments.

Surfactant-modified zeolite removed *Cryptosporidium* and *Giardia* surrogates from solution in the batch experiments with K_d values 10 to 20 times higher than those for zeolite or sand. This may be due to electrostatic and or hydrophobic interactions between the positively charged SMZ formulations and the negatively charged microspheres. However, column experiments did not show similar results. Based on column studies, all materials had relatively the same removal efficiencies in the range of 79.7(±1.6) to 82.3(±0.8)% for the *Cryptosporidium* surrogates and 99.1(±0.4) to 99.3(±0.1)% for the *Giardia* surrogates, which indicates that physical filtration or gravitational settling were the dominant mechanisms of removal rather than electrostatic or hydrophobic interactions.

INTRODUCTION

Microbial contamination of drinking water is a serious problem with global significance. *Cyrptosporidium parvum* and *Giardia intestinales (lamblia)* (Figure 1) are parasitic protozoa that exist in the environment as oocysts and cysts, respectively. Infectious (oo)cysts are shed in the feces of infected mammals including cattle and horses, and other domestic and wild animals such as migrating fowl. One gram of goose feces can yield 67 to 686 *Cryptosporidium* oocysts (Graczyk et al., 1998). Although dormant outside a host, as few as ten cysts can result in infection (Casemore et al., 1997). Their ubiquity in water around the world, coupled with their low infectious dose and resistance to chlorination, make *Cryptosporidium* and *Giardia* two of the most significant waterborne pathogens (Borucke, 2002). Cryptosporidiosis and Giardiasis are common gastrointestinal illnesses that occur from ingesting *Cryptosporidium* and *Giardia*. Symptoms include diarrhea, abdominal discomfort, nausea, and vomiting, among others (Girdwood, 1995). The illness is usually short-term for a healthy person, with a duration ranging from days to weeks. Among more vulnerable populations, gastrointestinal infection can be fatal. Vulnerable groups include children, the elderly, pregnant woman, and people with compromised immune systems.

Giardia is the more common cause of gastrointestinal disease with approximately 200 million cases of giardiasis reported worldwide every year (WHO, 1992), however,

Cryptosporidium often cause the most severe outbreaks (Addiss et al., 1995). The largest outbreak of cryptosporidiosis in the United States occurred in Milwaukee, Wisconsin in 1993. An estimated 403,000 people out of a population of 630,000 were either laboratory-confirmed for cryptosporidiosis or showed symptoms of infection including watery diarrhea (MacKenzie et al., 1994), which resulted in over 50 deaths (Hoxie et al., 1997).

As a consequence of the infectivity and effects of *Cryptosporidium* and *Giardia*, standards for such protozoa in drinking water are strict. U.S. EPA regulations require a maximum allowable concentration of zero oocysts per liter (U.S. EPA, 1998). Similarly, the World Health Organization holds that there is no tolerable concentration for microbial pathogenic to humans in drinking water (WHO, 1993). Impact on human health is especially pronounced for people in developing nations with inadequate water supplies and poor water treatment systems. Typical removal efficiencies of *Cryptosporidium* and *Giardia* for current water treatment technologies are shown in Table 1 (U.S. EPA, 1988). About 57-99% pathogen removal is achieved with coagulation, sedimentation and filtration. About 95% of all drinking water treatment systems use chlorination as the final treatment step for pathogens (Craun, 1993) however, *Cryptosporidium* and *Giardia* are resistant to chlorination (Korich et al., 1990) as well as hyper-chlorination. These pathogens have also been detected in water obtained through wells from groundwater sources. Since common treatment technologies do not completely eliminate these pathogens, it is important to develop a low maintenance, inexpensive system to effectively treat drinking water for *Cryptosporidium* and *Giardia*.

This study investigated the application of surfactant-modified zeolite (SMZ) in the treatment of *Cryptosporidium* and *Giardia*. The biological filter medium is a mined granular zeolite treated with a common surfactant found in hair conditioners and mouthwash. Surfactant-modified zeolites have been extensively studied for removal of neutral and anionic contaminants from water (Bowman et al., 2000), and *E. coli* and bacteriophages from sewage water (Schulze-Makuch et al., 2002, 2003). This inexpensive ($0.50/kg) SMZ has hydrophobic properties along with a positive surface charge that should bind neutral to negatively charged organisms such as *Cryptosporidium* and *Giardia*. Two different SMZ formulations were engineered and their surface properties characterized. Using laboratory batch and column experiments, the two SMZ formulations and surfactant-free raw zeolite were tested for adsorption of synthetic microsphere surrogates having size and charge characteristics similar to *Cryptosporidium* and *Giardia*.

MATERIALS AND METHODS

Material Properties

The sand used in this study (0.18-0.71 mm grain size) was the same material used in bench scale aquifer model experiments by collaborators at the University of Texas in El Paso, TX (T. Lehner, University of Texas, El Paso, personal communication, 2004). Sand is commonly used in water treatment technologies such as rapid and slow sand filtration (Table 1). The sand grain size was much finer than that of the zeolite used, and thus served as a comparative medium in the batch experiments and the mini-column experiments presented in Appendix C. Sand was not tested in the larger column

experiments since several pore volumes (PV) of input solution would be required to achieve minimal microsphere breakthrough, resulting in expense beyond the budget of this project.

The zeolite used in the study is a natural clinoptilolite-rich tuff obtained from the St. Cloud mine near Winston, NM. This zeolite alteration occurs in tuffaceous sediments and the tuff of Little Mineral Creek of the Santa Fe Formation, which dates back 29.0 Ma (Harrison, 1986, 1989; McIntosh et al., 1991). The mineral composition of an earlier sample from this deposit, based on internal standard XRD analysis (Chipera and Bish 1995; Sullivan et al., 1997) was 74% clinoptilolite, 5% smectite, 10% quartz/cristobalite, 10% feldspar, and 1% illite. The zeolite was crushed and sieved to a 1.4 to 2.4 mm (8-14 mesh) grain size. For this grain size, the surface area was 13.44 (±0.17) m^2/g (X. Tao, Chinese University of Geosciences, personal communication, 2001). Using the surfactant salt hexadecyltrimethylammonium-chloride (HDTMA-Cl), the hexadecyltrimethyl-ammonium (HDTMA) maximum surfactant loading (MSL) was previously reported to be 140 mmol HDTMA/kg zeolite (Bowman et al., 2000).

The MSL of the zeolite sample used in this study was determined by treating a known mass of zeolite with an excess amount of surfactant. The MSL was measured to be 87.2 mM HDTMA/kg zeolite, which is less than the amount reported by Bowman et al., (2000). Previous work (Li and Bowman, 1997) showed that when HDTMA-Cl is used, cationic SMZ forms when the surfactant loading reaches the MSL and hydrophobic SMZ forms when surfactant loading is equal to the cation exchange capacity or about ⅔MSL.

The surfactant used in the study was Lonza HDTMA-Cl Carsoquat solution (CT-429, Code No. 5330000618, Lot No. D8223090, CAS No. 112-02-7) which contains 29% by wt. HDTMA-Cl.

SMZ Preparation

The goal of this study was to prepare two different SMZ formulations (cationic SMZ and hydrophobic SMZ), which was easily accomplished by modifying the amount of surfactant loading on the surface of the zeolite. Treatment was accomplished through an up-flow system by placing 10 kg of zeolite in a 20-L plastic bucket that had barb fittings at the bottom and near the top, which served as inlet and outlet ports. The medium was saturating with CO_2 gas for 4 h to displace air. A 20-L volume of the appropriate surfactant solution was mixed and placed in a 20 L reservoir and then circulated through the medium at a flow rate of 60 mL/min using a CHEM-FEED pump (Blue White Industries, Westminster, CA). The initial HDTMA solutions were sampled and then after 24 h of circulation the equilibrium HDTMA solutions were sampled. The modified zeolite was rinsed with 10 PV of DI water and the rinse HDTMA solutions were sampled to ensure that all excess surfactant was removed. Upon treatment, the SMZ was air-dried under a fan for about 3 days.

The initial surfactant solution concentrations used to produce the cationic SMZ and hydrophobic SMZ were 58.9 mM HDTMA (117.8 mmol HDTMA/kg zeolite) and 33.3 mM HDTMA (66.6 mmol HDTMA/kg zeolite), respectively. The cationic SMZ had non-sorbed surfactant detected in the equilibrium solution (23.8 mmol HDTMA/kg zeolite) and three rinse solutions (5.2, 1.0, and 0.6 mmol HDTMA/kg zeolite). However, negligible amounts of surfactant were detected in the equilibrium solution (0.2 mmol

HDTMA/kg zeolite) and rinse solution (0.2 mmol HDTMA/kg zeolite) of the hydrophobic SMZ, which indicated that all the surfactant from the initial HDTMA solution was sorbed during the treatment process. The surfactant loading on each formulation was determined by subtracting the mass of HDTMA in the equilibrium and rinse solutions from the initial mass of HDTMA used for treatment. The surfactant loading on the cationic SMZ was equal to the MSL (87.2 mmol HDTMA/kg zeolite). However, the surfactant loading on the hydrophobic SMZ was about ¾MSL (66.2 mmol HDTMA/kg zeolite) instead of the targeted amount of ⅔MSL due to a calculation error during the preparation of the initial HDTMA solution.

The HDTMA solution concentrations were analyzed using high performance liquid chromatography (HPLC), which consisted of a Waters 501 HPLC Pump, Waters 717 plus Autosampler, Waters UV 486 Tunable Absorbance Detector (265 nm wavelength) and EZChrom Elite software all from Waters Corporation (Milford, MA). Samples were run using 25-µL injections into a 5-mM p-toluenesulfunate and methonal (45:55) by volume mobile phase solution. Chromatographic separation was achieved with a 150 mm x 4.6 mm Nucleosin CN 5-µm column (Supelco, Bellefonte Park, PA) after 3 min at a pump flow rate of 1 mL/min.

Characterization of SMZ and Zeolite Surface Properties

Twenty-grams of cationic SMZ, hydrophobic SMZ, and untreated zeolite were crushed and placed in a glass bottles. Each medium was shaken with 40 mL of DI water, and then allowed to sit. After 2 h the samples were visibly inspected (see Appendix Figure D-3). The cationic SMZ and zeolite samples had visible particles remaining in suspension, which indicated that the particles were charged and repelling each other

electrostatically. The hydrophobic SMZ sample, however, did not have visible particles in suspension, which indicated that the particles were less repulsive and were able to aggregate.

To further analyze surface properties of each medium, hydrophobicity and net surface charge of the cationic SMZ, hydrophobic SMZ and zeolite were measured. The hydrophobicity of the surface was determined by contact angle measurements in air using the drop technique (Gaudin et al., 1963) with water as the wetting fluid. Four grains of each medium were chosen for analysis based on large size and flatness of shape. Average contact angles through the water phase for cationic SMZ and hydrophobic SMZ were $54^{o}(\pm 3)$ and $126^{o}(\pm 5)$, respectively. These measurements indicate hydrophilic and hydrophobic surface properties for each medium, respectively. Contact angles for untreated zeolite were about 0^{o}. Since a stable water drop could not be placed on the zeolite grain surface, this indicates fully wetting hydrophilic surface properties for the zeolite medium. These measurements give an idea of the hydrophobicity of each medium however, due to the small particles size and resultant surface roughness, they may not be exact.

Electrophoretic mobility was used to evaluate the net surface charge of each medium by measuring zeta potentials with a Coulter DELSA 440SX (Becton Coulter Co, Hialeah, FL). Cationic SMZ, hydrophobic SMZ, or zeolite particles were crushed and mixed with DI water to prepare 10 mL (0.1% by wt.) samples. The samples had a pH of about 7.4 and conductivity between 0.204 to 0.298 mS/cm. The samples were placed in a flow cell and the zeta potential values were recorded. The cationic SMZ and hydrophobic SMZ formulations both had net positive zeta potentials of +44.75 and +43.85 mV,

respectively. The raw zeolite had a net negative surface charge of -28.1 mV. These measurements give an idea of the surface charge in terms of positive and negative zeta potential but may not be exact since there was substantial particle settling observed within the flow cell during measurements.

Interestingly, the zeta potentials of the two SMZ formulations were quite similar. Past research (Li and Bowman, 1998) has shown similar zeta potentials for the cationic SMZ, however a near neutral zeta potential for the hydrophobic SMZ. The hydrophobic SMZ had both hydrophobic contact angle and a positive zeta potential, which indicates partial monolayer/bilayer HDTMA coverage. This results when the surfactant loading is above the external cation-exchange capacity (>⅔MSL) but below the MSL (Yeskie and Harwell, 1998), as was the case for the hydrophobic SMZ, which had ¾MSL.

Pathogen Surrogates

Due to the low infectious does of live pathogens and difficulty of handling, Dragon Green ® fluorescent-dyed polystyrene microspheres with carboxylate functional groups (Bangs Laboratories, Inc., Fishers, IN) were used as surrogates for both *Cryptosporidium* oocysts and *Giardia* cysts. Polystyrene microspheres with carboxylate functional groups are commonly used in research as surrogates for pathogens (Dai and Hozalski, 2003).

Cryptosporidium oocysts are almost spherical with a diameter of 4.5-5.5-μm (Medema et al., 1998) and have neutral to slightly negative surface charge (Brush et al.; 1998, Drozd and Schwartzbrod, 1996) with a zeta potential of -1.5 to -12.5 mV at a pH of 6.7 (Dai and Hozalski, 2003). The mean diameter of the microspheres for the *Cryptosporidium* surrogates was 5.01 μm (±0.14). Provided by the manufacture, the

surface charge expressed as surface titration was 4.1 μeq/g and the particle density was 1.1 g/mL.

Giardia cysts are oval-shaped with a diameter of 9-12 μm (Tufenkji et al., 2002) and have a net negative surface charge with a zeta potential of -34.31 mV at pH 7.3 (Ongerth and Pecoraro, 1996). The mean diameter of the microspheres for the *Giardia* surrogates was 10.43 μm (±1.09). According to the data provided by the manufacture, the surface charge expressed as surface titration was 5.0 μeq/g and the particle density was 1.06 g/mL.

The net charge on the 5- and 10-μm microspheres was determined by using the same electrophorectic mobility test and sample preparation as described above, however no crushing was required. The samples had a pH of about 7.4 and conductivity between 0.177 to 0.862 mS/cm. The 5- and 10-μm microspheres had average zeta potentials of -25.00 and -17.25 mV, respectively. These measurements also give an idea of the surface charge but may not be exact since there was also substantial particle settling observed within the flow cell during measurements. Past research (Dai and Hozalski, 2003) of fluorescent latex microspheres (Polysciences Inc., Warrington, PA) as surrogates for *Cryptosporidium* has shown a wide range of zeta potential values from -7.4 to -50.2 mV depending on calcium concentration. Dai and Hozalski (2003) concludes that although the microspheres may be more negatively charged than actual *Cryptosporidium* organisms, they could still serve as conservative surrogates for determining oocyst removal in filtration experiments.

Microsphere concentrations in solution were measured using flow cytometry (FC) (FACScan Analzer Immunocytometry System, Becton Dickenson, San Jose, CA),

which has been used by many researchers for enumerating bacterial cells and microspheres (Stewart and Steinkamp, 1982; Molema et al., 1998; Fuller et al., 2000; DeFlaun et al., 2001). The lower detection limit for the microspheres used in this study was about $1x10^3$ cpm/mL. A detailed description of FC method and procedures for analyzing the microsphere surrogates is presented in Appendix A.

Microsphere Sorption in Batch Experiments

Duplicate batch experiments were conducted on cationic SMZ, hydrophobic SMZ, zeolite, and sand by combining 10 g of material with 20 mL of microsphere solution. The solutions contained both 5- and 10-µm microspheres with concentrations varying from 10^3 to 10^5 microspheres/mL. Samples were placed in 50-mL glass scintillation vials (Fisher Scientific, Denver, CO) and were mixed at 100 rpm for 8 h at 25°C. Four-milliliters of initial and equilibrium solutions were removed, filtered with 30-µm filters to remove medium solids, placed in 5-mL falcon tubes (Becton Dickenson, Fisher Scientific, Denver, CO), sonciated, and analyzed using FC.

Microsphere Sorption in Laboratory Columns

Six vertical columns made of acrylic plastic (Soil Measurement Systems, Tucson, AZ) with a 2.54-cm inner diameter and 15-cm length were packed with cationic SMZ, hydrophobic SMZ and zeolite. Within the endplates 30-µm nylon screens were used to retain the medium within the columns and filter the effluent samples for analysis. Three-way check valves (Cole-Palmer, Vernon Hills, IL) were connected to the ends of each column with Luer fittings. These valves served as sample ports and sealed the columns shut between experiments. Once packed, the columns were purged with CO_2 for 4 h and

were then saturated from the bottom with degassed synthetic water at a flow rate of 0.9 mL/min using a multichannel syringe pump (KDScientific Inc., New Hope, PA). The synthetic water was made using 300 mg/L NaCl and Type I water (purified with a Milli-Q system, Millipore Corp., Bedoford, MA). The columns were assumed to be at steady state when no gas bubbles were visible and the water-filled column weights remained constant. The PV was calculated after measuring the dry and saturated weights of each column.

A 2-PV slug of tritiated water tracer (tritium) with a specific activity of $2x10^4$ cpm/mL was injected into each column to determine the flow velocity and column dispersion coefficient. Effluent samples were collected every 0.2 PV in 20-mL glass scintillation vials using Retriever II fraction collectors (ISCO Inc., Lincoln, NE). One-milliliter of effluent solution was combined with 5 mL of scintillation cocktail solution (ICN Biomedicals, Inc., Irvine, CA) for analysis with an LS6500 liquid scintillation counter (Beckman Coulter, Inc., Fullerton, CA).

Microsphere transport experiments were then conducted through the same packed columns. Input concentrations of 10^5 microspheres/mL of each size were continuously injected at a flow rate of 0.9 mL/min. Four-milliliter effluent samples were collected continuously in 5-mL falcon tubes using Retriever II fraction collectors. Input and effluent microsphere samples were sonicated and then analyzed using FC.

After the column experiments were conducted and the pore fluid drained, the medium from columns Zeolite 1 and Zeolite 2 were removed, sectioned into fifths from the bottom up and placed in Petri dishes to dry. The nylon screens of each column was also removed and placed in Petri dishes to dry, however were lost up a fume hood during

drying. The samples were visually inspected under an Ultraviolet Transilluminator (Ultra-Lum Inc., Carson, CA) for microsphere distribution within the media.

RESULTS AND DISCUSSION

Batch Experiments Data

Batch experiment data for each medium are presented in Figures 2 and 3. The batch experiments were fit with linear adsorption isotherms on normal-normal and log-log plots using equations:

$$S = K_d C_e^{\,N} \qquad (1)$$

$$\mathrm{LOG}(S) = \mathrm{LOG}(K_d) + N\,\mathrm{LOG}(C_e) \qquad (2)$$

where S is the concentration of species adsorbed on the solid phase (M/M), K_d is the linear equilibrium coefficient (partitioning coefficient) (L^3/M), C_e is the equilibrium solution concentration (M/L^3) and N is a constant equal to 1 for linear adsorption isotherms.

All isotherms for Figures 2a and 3a showed linearity with R^2 values ranging from 0.729 to 0.997 (Table 2). All isotherms for Figures 2b and 3b also showed linearity with N values close to 1 ranging from 0.82 to 1.12 and R^2 values ranging from 0.863 to 0.981. Linear distribution coefficients for the different materials and microspheres ranged from 104 to 2020 mL/g for the 5-µm microspheres and 2.0 to 24.3 mL/g for the 10-µm microspheres. Cationic SMZ and hydrophobic SMZ yielded 10-20 times higher K_d values than zeolite and sand, with more 5- than 10-µm microspheres sorbed in all cases. This may have been due to electrostatic and or hydrophobic interactions between the positively charged SMZ formulations and the negatively charged microspheres. The

Cryptosporidium surrogates had a slightly more positive zeta potential than the *Giardia* surrogates and could have adsorbed more strongly to the materials.

Tritium BTC Data from Column Experiments

The tritium BTCs for the columns were well described by the 1-dimensional advection-dispersion equation:

$$R\frac{\partial C^*}{\partial PV} = \frac{1}{P}\frac{\partial^2 C^*}{\partial X^2} - \frac{\partial C^*}{\partial X} \quad (3)$$

where:

$$C^* = \frac{C}{C_o} \quad (4)$$

$$P = \frac{vL}{D} \quad (5)$$

$$R = 1 + \left(\frac{\rho}{\theta}\right)K_d \quad (6)$$

$$PV = \frac{vt}{L} \quad (7)$$

$$X = \frac{x}{L} \quad (8)$$

and C is the effluent solute concentration (M/L^3), C_o is the influent solute concentration (M/L^3), C^* is the dimensionless solute concentration, D is the dispersion coefficient (L^2/T), v is the pore-water velocity (L/T), x is the distance (L), L is the column length (L), PV is dimensionless time (pore volumes), ρ is bulk density (M/L^3), θ is volumetric water content, P is the Peclet number, and R is the retardation factor, and X is the dimensionless length.

Equation 3 was fitted to the observed tritium data using the nonlinear, least-squares optimization program CXTFIT 2.1 with flux-type boundary conditions (Toride et al., 1999). The pore-water velocity *v* was treated as a fixed value and *R* and *D* were fitted. The tritium BTC for Cationic SMZ 1 is shown in Figure 4. All six columns yielded similar tritium BTCs with symmetrical shapes and *R* values in the range 1.13 to 1.23 (Table 3). This indicates that the columns were well packed resulting in uniform flow and minimal fluid channeling.

Microsphere BTC Data from Column Experiments

Removal efficiency for packed filter beds is commonly quantified using the following equation:

$$\textit{Removal Efficiency} = \left(1 - \frac{C}{C_o}\right) \times 100 \qquad (9)$$

where removal efficiency is in terms of percent, and *C* is the average effluent solute concentration.

Microsphere BTC data was plotted for all six columns as C/C_o vs PV. Equation 9 was used to determine column removal efficiencies from the plotted data. The microsphere BTCs for Cationic SMZ 1, Hydrophobic SMZ 1, and Zeolite 1 are all plotted in Figures 5 and 6. Table 4 lists the removal efficiencies for each column. All six columns yielded similar removal efficiencies in the range 77.0(±0.8) to 82.3(±0.8)% for the 5-µm microspheres and 98.8(±0.4) to 99.3(±0.1)% for the 10-µm microspheres. Column experiment data suggest that there was no preferential removal of microspheres among the three materials tested and that there was a higher removal of *Giardia* surrogates than *Cryptosporidium* surrogates for all materials. This data is not consistent

with the observations from the batch experiments where cationic SMZ and hydrophobic SMZ preferentially adsorbed the microspheres and K_d values for *Cryptosporidium* surrogates were greater than for *Giardia* surrogates. Clearly, different mechanisms of removal were taking place in the batch and column experiments.

Since the cationic SMZ, hydrophobic SMZ, and zeolite all had the same grain size distribution, the microsphere removal that was achieved in the column experiments may be due to physical filtration. This would explain the consistency among removal efficiencies of the different media and the fact that the larger *Giardia* surrogates were more successfully removed than the smaller *Cryptosporidium* surrogates by all media. The microspheres are slightly denser than water and may have gravitationally settled within the columns, however, preliminary studies of minimum flow rate were conducted to minimize this effect (see Appendix A for a more detailed description of the minimum flow rate selected). Dai and Hozalski (2003) conducted similar column experiments in which they used latex microsphere surrogates to simulate *Cryptosporidium* removal through 0.55-mm spherical glass bead medium. They achieved microsphere removal efficiencies ranging from 13.7 to 69.3%, for various concentrations of $CaCl_2$ and the presence of absence of natural organic matter. Greater removal may have been achieved during the current study due to the surface roughness and irregular grain shapes of the SMZ and zeolite materials used.

When the Zeolite 1 and Zeolite 2 column media were observed under ultraviolet light, most of the microspheres were in the bottom two-fifths of the columns near the inlet, with few-to-no microspheres visibly observed in the top three-fifths of the columns (see Appendix Figure D-11). This further strengthens the idea that microspheres were

physically filtered or gravitationally settled out within the media and that after 10 PV the bulk microsphere front had not reached the outlet of the columns.

It is possible that microspheres in the column experiments may have been subject to hydrodynamic forces (e.g., lift or drag forces resulting from the fluid flow in the porous media), which tend to detach previously attached colloids from collector surfaces. However, this is not believed to be the case here. Effective pore velocities needed for detachment to occur have been observed by Bergendahl and Grasso (2000) on the order of tens of centimeters/minute. The velocities used in this study ranged from 0.25 to 0.29 cm/min.

It is important to note that physical filtration of the microspheres may have occurred through the 30-μm screens, which were used in both the batch and column experiments to filter samples prior to FC analysis. However, this would not explain the preferential sorption observed in the batch experiments between the different types of medium. Prior to analysis, filtering the samples was required since the FC could have been clogged and damaged by particles larger than 35 μm.

CONCLUSIONS

Laboratory batch experiments showed that cationic SMZ and hydrophobic SMZ preferentially remove *Cryptosporidium* and *Giardia* surrogates from solution with K_d values 10 to 20 time higher than those for surfactant-free zeolite and sand. This indicates that the negatively charged microspheres electrostatically and/or hydrophobically adsorbed to the cationic SMZ and hydrophobic SMZ materials. Clearly there is an

affinity of *Cryptosporidium* and *Giardia* surrogates to the SMZ formulations, however zeta potentials of live *Cryptosporidium* and *Giardia* organisms are not as negatively charged as the surrogates used in this experiment. Batch experiments should be conducted with live organisms to determine, if under more realistic conditions, similarly favorable K_d values can be obtained for these SMZ formulations.

If the batch experiments prove successful with live organisms then additional research should be conducted to investigate if an efficient and cost effective treatment method can be engineered to enhance removal from drinking water. Current technologies remove 57-99% of pathogen from drinking water, however, it is the remaining percentage of organisms not removed that can prove infectious. The column experiments did not prove that SMZ filtration is more efficient than what is currently achieved with coagulation, sedimentation or filtration technologies. Among the different materials tested in the column experiments, there was no preferential removal of microsphere surrogates which indicated that the removal mechanisms may have been dominated by physical filtration or gravitational settling instead of electrostatic or hydrophobic interactions. Recommendations for future work include investigating the use of crushed SMZ as a coagulant for pathogens which could then be settled out or filtered as a polishing technique. Down-flow SMZ column experiments could also be conducted to determine if better removal can be achieved by utilizing all four of the removal mechanism observed: physical filtration, gravitational settling, electrostatic and hydrophobic adsorption.

APPENDIX I. REFERENCES

Addiss, D.G., MacKenzie, W.R., Hoxie, J.J., Graus, M.S., Blair, K.A., Proctor, M.E., Kazmierczak, J.J., Schell, W.L., Osewe, P., Frisby, H. Cicerello, Cordell, R.L., Rose, J.B., and Davis, J.P. 1995. "Epidemiologic features and implications of the Milwaukee cryptosporidiosis outbreak, protozoan parasites and water." *The Royal Society of Chemistry*, Cambridge: pp. 19-25.

Bergendahl, J., Grosso, D. 2000. "Prediction of colloid detachment in a model porous media: hydrodynomics." *Chemical Engineering Science* 55(2000) 1523-1532.

Borucke, M.J. 2002. "Filtration of giardia cysts from Haitian drinking water." Massachusetts Institute of Technology.

Bowman, R.S., Sullivan, E.J., Li, Z. 2000. "Uptake of cations, anions, and nonpolar organic molecules by surfactant-modified Clinoptilolite-rich tuff." Colella, C., Mumpton, F.A., eds., Natural Zeolites for the Third Millennium, De Frede editore, Naples, Italy, pp. 287-297.

Brush, C.F., Walter, M.F., Anguish, L.G., Ghiorse, W.C. 1996. *Appl. Environ. Microbiol*. 64, 4439-4445.

Casemore, D.P., Wright, S.E., and Coop, R.L. 1997. "Cryptosporidium and cryptosporidiosis." Fayer, R., Ed.; CRC Press: Boca Raton, FL, pp 65-92.

Chipera, S.J., and Bish, D.L. 1995. "Multireflection RIR and intersity normalizations for quantitative analysis: Applications to feldspars and zeolites." *Power Diffract*., 10, 47-55.

Craun, G.F. 1993. "Safety of Water Disinfection: Balancing Chemical and Microbial Tisks." ILS1 Press, Washington, D.C.

Dai, X., Hozalsk, R.M. March 2003. "Evaluation of microspheres as surrogates for Cryptosporidium Parvum oocysts in filtration experiments." *Environ Sci Technol*. 1;37(5):1037-42.

DeFlaun, M.F., Fuller, M.E., Zhang P., Johnson, W.P., Mailloux, B.J., Holben, W.E., Kovacik, W.P., Balkwill, D.L., and Onstott, T.C. 2001. "Comparison of methods for monitoring bacterial transport in the subsurface." *J. Microbiol. Methods*., 47(2), 219-231.

Drozd, C., Schwartzbrod, J. 1996. Appl. Environ. Microbiol. 62, 1227-1237.

Fuller, M.E., Streger, S.H., Rothmel R.K, Mailloux, B.J., Hall, J. A., Onstott, T.C., Fredrickson, J.K., Balkwill, D.L., and DeFlaun, M.F. 2000. "Development of a vital fluorescent staining method for nomitoring bacterial transport in subsurface environments." *Appl. Environ. Microbiol*., 66(10), 4486-4496.

Gaudin, A.M., Witt, A.F., and Decker, T.G. March, 1963. "Contact angle hysteresis-principles and applications of measurement methods." Trans., AIME, 107-112.

Girdwood, R.W.A. 1995. "Some clinical perspectives on waterborne parasitic protozoa, protozoan parasites and water". The Royal Society of Chemistry, Cambridge. pp. 3-9.

Graczyk, T.M., Fayer, R., Trout, J.M, Lewis, E.J, Farley, C.A, Sulaiman, I., and Lal, A.A. 1998. "Giardia sp. cysts and infectious cryptosporidium parvum oocysts in the feces of migratory canada geese (Branta Canadenses)." *Appl. Environ. Microbiol*. 64:2736-2795.

Harrison, R.W. 1986. "General geology of Chloride Mining District, Sierra and Catron counties, New Mexico," New Mexico Geological Society, Guidebook 37, pp. 265-272.

Harrison, R.W. 1989. "Geology of Winston 7½ -minute quadrangle, Sierra County, New Mexico." New Mexico Bureau of Mines and Mineral Resources, Openfile Report 358, 17 pp., 2 sheets, scale 1:24,000.

Hoxie, N.J., Davis, J.P., Vergeront, J.M., Nashold, R.D., and Blair, K. A. 1997. "Cryptosporidiosis-associated mortality following a massive waterborne outbreak in Milwaukee, WI." *Am. J. Public Health* 87, 2032-2035.

Korich, D.G., Mead, J.R., Madore, M.S., Sinclair, N.A. and Sterling, C.R. 1990. 'Effects of Ozone, Chlorine Dioxide, Chlorine, Monochloramine on Crytosporidium Parvum Oocysts Viability." *Appl. Environ. Microbiol*. 56, 1423-1428.

Li, Z., and Bowman, R.S. 1998. "Sorption of Perchloroethylene by Surfactant-Modified Aeolite as Controlled by Surfactant Loading." *Environ. Sci. Technol*. 32(15) 2278-2282.

Li, Z., and Bowman, R.S. 1997. "Counterion effects on the sorption of cationic surfactant and chromate on natural clinoptilolite." *Environ. Sci. Technol*. 31:2407-2412.

Lindquist, H.D.A. (April 2004) U.S. EPA (http://images.google.com/images?q=H.D.A.%20Lindquist%2C%20U.S.%20EPA&hl=en&lr=&ie=UTF-8&oe=UTF-8&sa=N&tab=wi)

MacKenzie, W., Hoxie, N., Proctor, M., Gradus, M., Blair, K., Peterson, D., Kazmierczak, J., Addiss, D., Fox, K., Rose, J., and Davis, J. 1994. "A massive

outbreak in Milwaukee of Cryptosporidium infection transmitted through the public water supply. *The New England Journal of Medicine*, 331: 161-167.

McIntosh, W.C., Kedzie, L.L., Sutter, J.F. 1991. "Paleomagnetism and 40Ar/39Ar ages of ignimbrites, Mogollon-Datil Volcanic Field, southwestern New Mexico." New Mexico Bureau of Mines and Mineral Resources, Bulletin 154, pp. 112-120.

Medema, G.J., Schets, F.M., Teunis, P.F.M., Havelaar, A.H. 1998. *Appl. Environ. Microbiol.* 64, 4460-4466.

Molema, G., Mesander, G., Kroesen, B., Helfrich, W., Meijer, D., and de Leij, L. 1998. "Analysis of in vitro lymphocyte adhesion and transendothelial migration by fluorescent-beads-based flow cytometric cell counting." *Cytometry*, 32, 37-43.

Ongerth, J.E. and Pecoraro, J.P., March, 1996. Electrophoretic Mobility of Cryptosporidium Oocysts and Giardia Cysts." *Journal of Environmental Engineering*, 122(3); pp. 228-231.

Schulze-Makuch, D., Pillai, S.D., Guan, H., Bowman, R., Couroux, E., Hielscher, F., Totten, J., Espinosa, I.Y., and Kretzschmar, T. 2002. "Surfactant-modified zeolite can protect drinking water wells from viruses and bacteria, *EOS*, 83(193-201).

Schulze-Makuch, D., Bowman, R.S., Pillai, S.D., and Guan, H. 2003. "Field evaluation of the effectiveness of surfactant modified zeolite and iron-oxide-coated sand for removing viruses and bacteria from ground water." In review at *Ground Water*.

Stewart, C., and Steinkamp, J. 1982. "Quantification of cell concentration using the flow cytometer." *Cytometry*, 2, 238-243.

Sullivan, E.J., Hunter, D.B. and Bowman, R.S. 1997. "Topological and thermal properties of surfactant-modified clinoptilolite studied by tapping-mode atomic force microscopy and high-resolution thermogravimetric analysis." *Clays Clay Miner*., 45(1), 42-53.

Toride, N., Leij, F.J., and van Genuchten, M.T. 1999. "The CXTFIT code for estimating transport parameters from laboratory or field tracer experiments, version 2.1." Research Report No. 137 U.S. Salinity Laboratory, USDA, ARS, Riverside, CA.

Tufenkji, N., Ryan, J.N., Elimelech, M. 2002. *Environ. Sci. Technol*. 36, 422A-428A.

U.S. EPA 1988. "Comparative health effects assessment of drinking water treatment Technologies." Office of Drinking Water U.S. Environmental Protection Agency, Washington, D.C.

U.S. EPA December, 1998." United States Environmental Protection Agency, interim enhanced surface water treatment rule, Federal Register Document." (http://www.epa.gov/safewater/mdbp/ieswtrfr.html)

WHO. 1993. "World Health Organization, Water and sanitation: guidelines for drinking water quality (accessed 5.20.2002)." (http://www.who.int/water_sanitation_health/GDWQ/Microbiology/GWDWQMicrobiological2.html)

WHO. 1992. "*Global health situation and projections--estimates*." (accessed 4.14.2004)." (http://www.ciesin.org/docs/001-010/001-010c.html)

Yao, K.M., Habibian, M.T. and O'Melia, C.R. 1971. "Water and wastewater filtration: concepts and applications." *Environ. Sci. Technol.* 5: pp. 1105-1112.

Yeskie, M.A., and J.H. Harwell. 1998. "On the structure of aggregates of adsorbed surfactants: The surface charge density at the hemimicelle/admicelle transition." *J. Phys. Chem*. 92:2346-2352.

Table 1. Typical removal efficiencies of *Cryptosporidium* and *Giardia* for current water treatment technologies (U.S. EPA, 1988).

Organisms	Coagulation and sedimentation (% removal)	Rapid filtration (% removal)	Slow sand filtration (% removal)
Total coliforms	74–97	50–98	>99.999
Fecal coliforms	76–83	50–98	>99.999
Enteric viruses	88–95	10–99	>99.999
Giardia	58–99	97–99.9	>99
Cryptosporidium	90	99–99	99

Table 2. Batch Experiment values for the microsphere sorption isotherms.

	(Equation 1)		(Equation 2)		
	K_d	R^2	N	LOG (K_d)	R^2
5-µm microspheres (*Cryptosporidium*)					
Cationic SMZ	2020	0.962	1.05	3.11	0.863
Hydrophobic SMZ	1290	0.729	0.87	3.39	0.953
Zeolite	137	0.997	0.92	2.30	0.975
Sand	104	0.997	0.95	2.12	0.981
10-µm microspheres (*Giardia*)					
Cationic SMZ	24.3	0.841	1.12	0.83	0.958
Hydrophobic SMZ	19.0	0.987	0.90	1.71	0.912
Zeolite	3.7	0.988	0.89	0.93	0.943
Sand	2.0	0.991	0.82	0.95	0.918

Table 3. Hydrodynamic characteristics of laboratory columns.

	Media Mass (g)	**Pore Volume (mL)**	***R***	***P***	**θ**	**ρ (g /cm^3)**
Cationic SMZ 1	66.5	51.3	1.17	411	0.68	0.875
Cationic SMZ 2	65.8	48.6	1.23	425	0.64	0.866
Hydrophobic SMZ 1	68.0	47.0	1.19	417	0.62	0.895
Hydrophobic SMZ 2	66.9	53.1	1.15	369	0.70	0.880
Zeolite 1	67.9	54.2	1.13	364	0.71	0.893
Zeolite 2	63.7	51.9	1.14	361	0.68	0.838

Table 4. Removal efficiencies of microspheres for each column.

	5 µm			10 µm		
	% Removal	**Ave**	**Std Dev**	**% Removal**	**Ave**	**Std Dev**
Cationic SMZ 1	80.9	79.7	1.6	99.2	99.2	0.1
Cationic SMZ 2	78.6			99.3		
Hydrophobic SMZ 1	77.6	77.0	0.8	99.3	99.1	0.4
Hydrophobic SMZ 2	76.4			98.8		
Zeolite 1	81.7	82.3	0.8	99.2	99.3	0.1
Zeolite 2	82.9			99.4		

FIGURE CAPTIONS

Figure 1. ***Cryptosporidium Parvum*** **oocysts and** ***Giardia Intestinales (Lamblia)*** **cysts (Lindquist, U.S. EPA).**

Figure 2. **Batch experiment observed data for 5-µm microspheres (*Cryptosporidium*) plotted as (a) *S* vs C_e with (Eq. 1) linear fit through zero (b) LOG(*S*) vs LOG(C_e) and (Eq 2) linear fit.**

Figure 3. **Batch experiment observed data for 10-µm microspheres (*Giardia*) plotted as (a) *S* vs C_e with (Eq. 1) linear fit through zero (b) LOG(*S*) vs LOG(C_e) and (Eq 2) linear fit.**

Figure 4. **Observed and fitted (Eq. 2) breakthrough curves for tritiated water in column Cationic SMZ 1.**

Figure 5. **Observed microsphere breakthrough curves for 5-µm microspheres (*Cryptosporidium*) of Cationic SMZ 1, Hydrophobic SMZ 1, and Zeolite 1.**

Figure 6. **Observed microsphere breakthrough curves for 10-µm microspheres (*Giardia*) of Cationic SMZ 1, Hydrophobic SMZ 1, and Zeolite 1.**

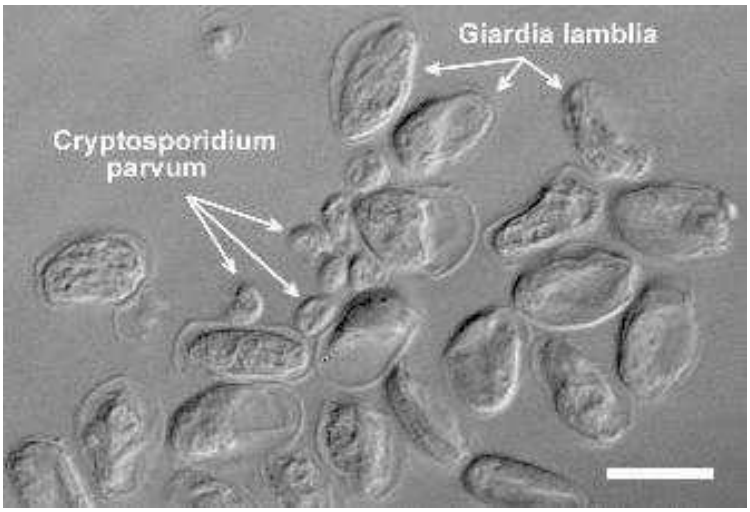

Figure 1. ***Cryptosporidium Parvum*** **oocysts and** ***Giardia Intestinales (Lamblia)*** **cysts (Lindquist, U.S. EPA).**

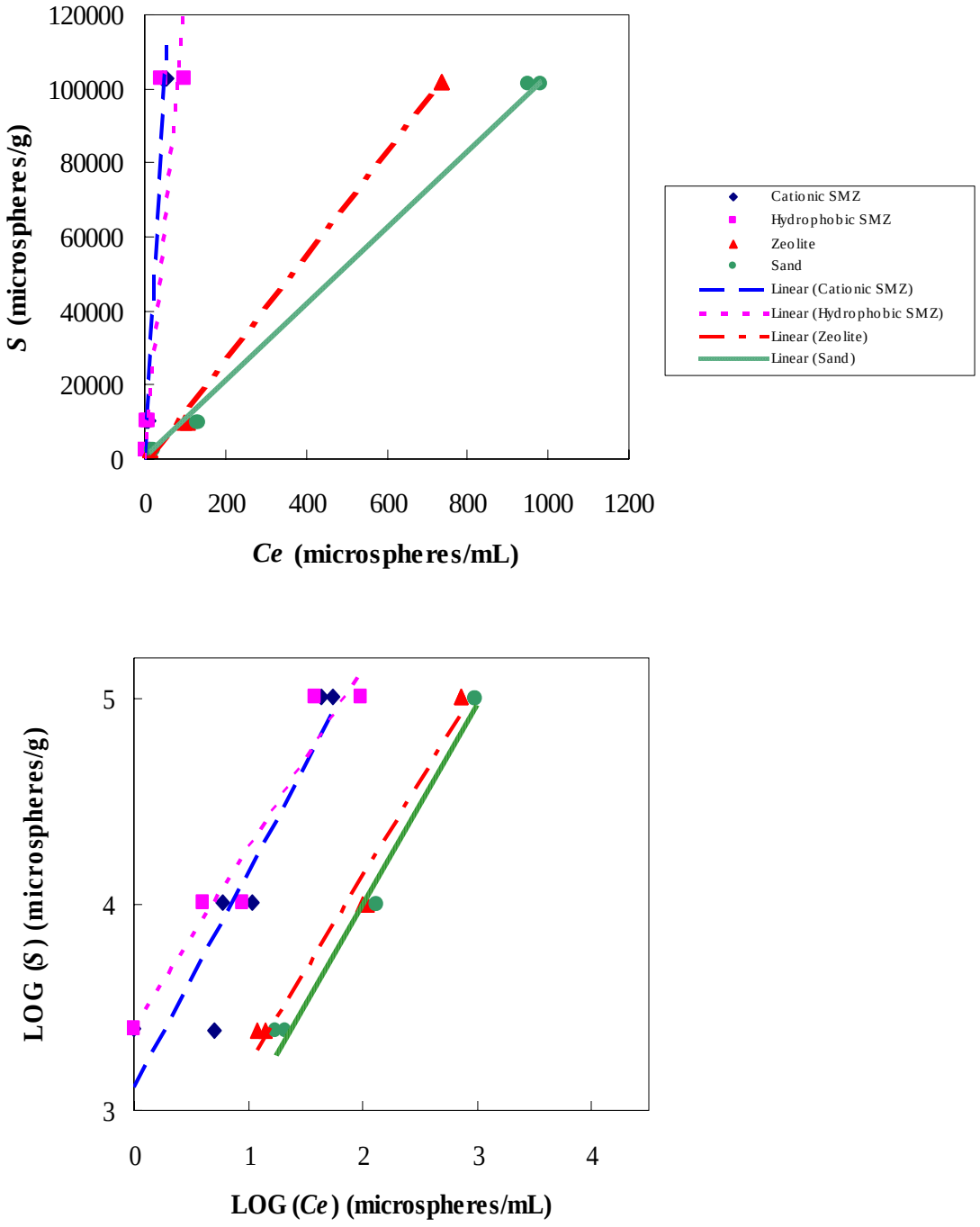

Figure 2. **Batch experiment observed data for 5-µm microspheres (*Cryptosporidium*) plotted as (a) *S* vs C_e with (Eq. 1) linear fit through zero (b) LOG(*S*) vs LOG(C_e) and (Eq 2) linear fit.**

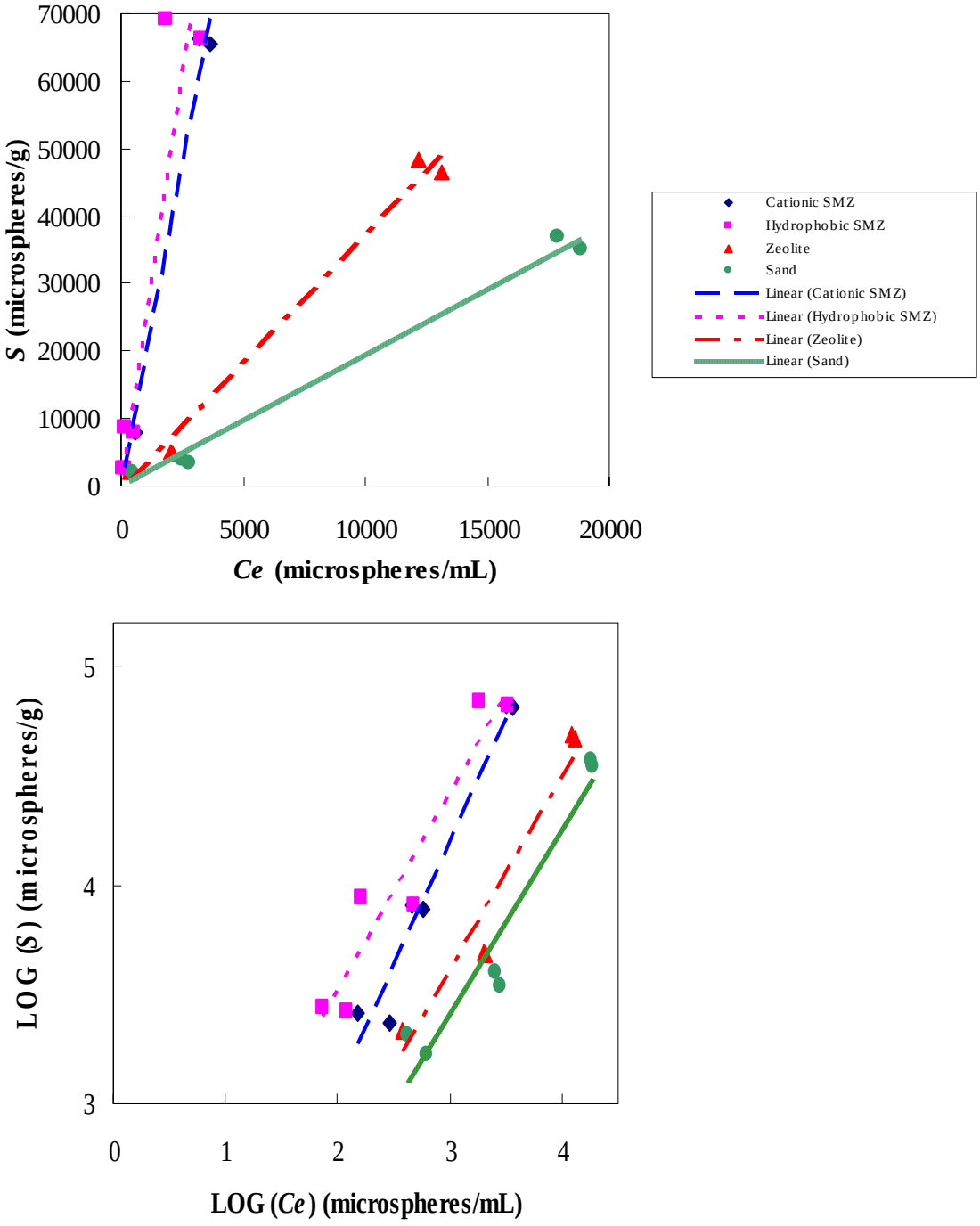

Figure 3. **Batch experiment observed data for 10-µm microspheres (*Giardia*) plotted as (a) *S* vs C_e with (Eq. 1) linear fit through zero (b) LOG(*S*) vs LOG(C_e) and (Eq 2) linear fit.**

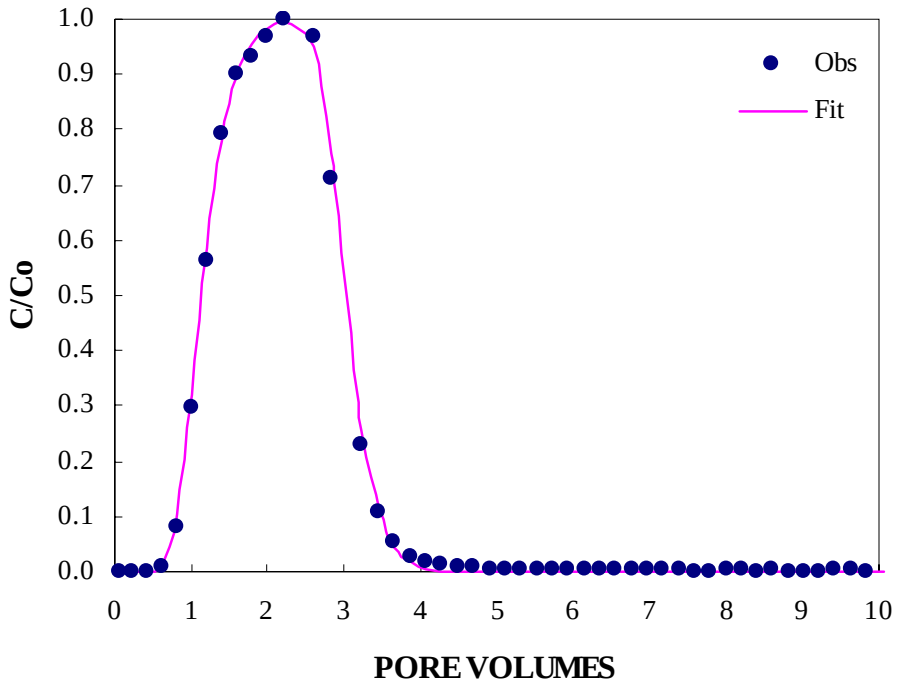

Figure 4. **Observed and fitted (Eq. 2) breakthrough curves for tritiated water in column Cationic SMZ 1.**

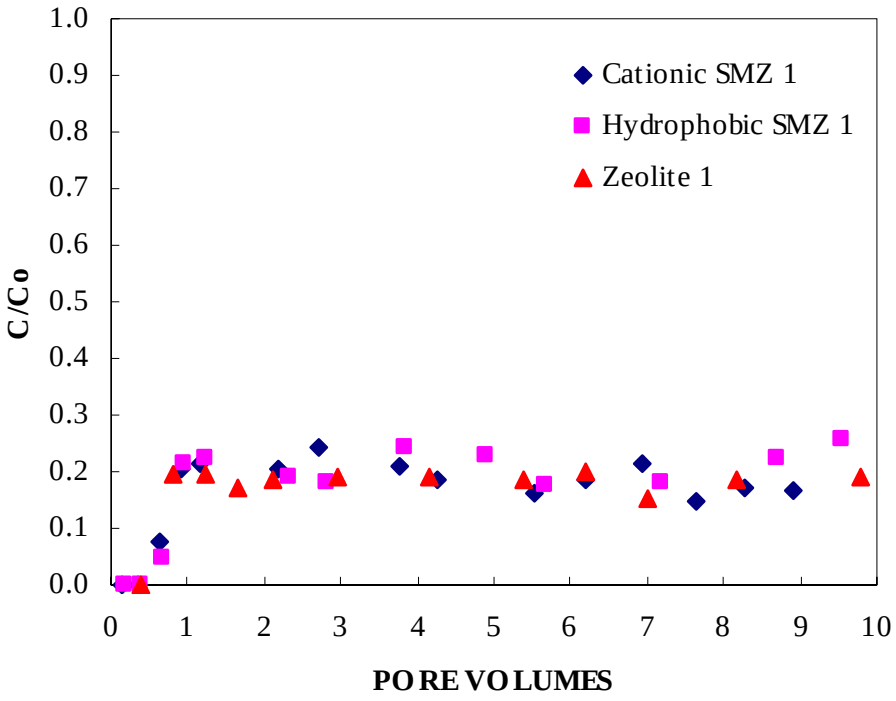

Figure 5. **Observed microsphere breakthrough curves for 5-µm microspheres (*Cryptosporidium*) of Cationic SMZ 1, Hydrophobic SMZ 1, and Zeolite 1.**

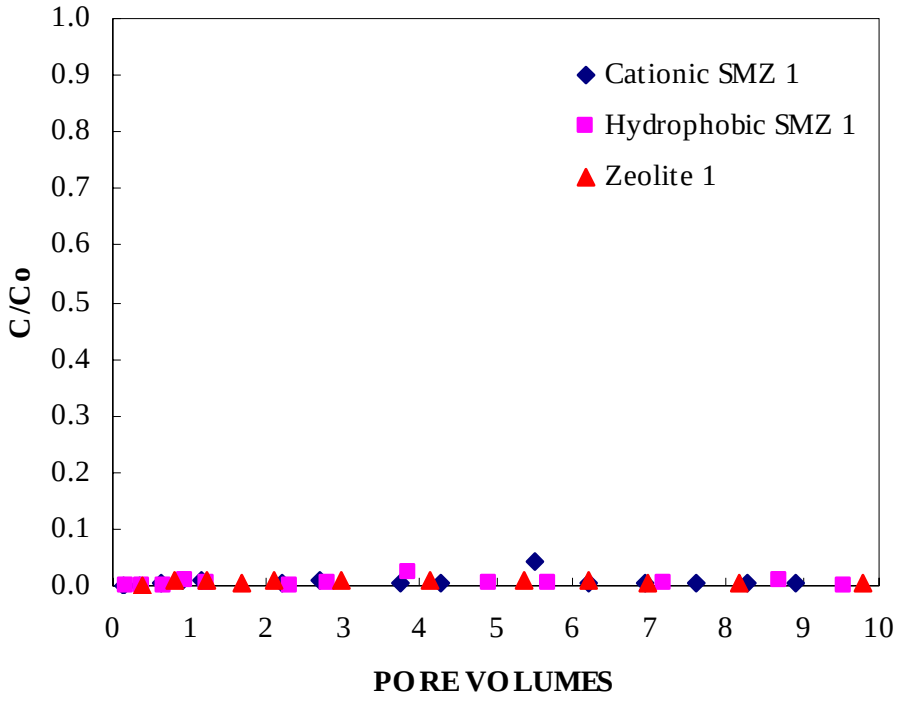

Figure 6. **Observed microsphere breakthrough curves for 10-µm microspheres (*Giardia*) of Cationic SMZ 1, Hydrophobic SMZ 1, and Zeolite 1.**

INTRODUCTION TO APPENDICES

The following appendices provide descriptions of preliminary and unreported studies, further information on methods used, and the experimental data collected throughout the thesis project.

Appendix A contains a detailed description of method and procedures for analyzing the microsphere surrogates using flow cytometry. Also included is the microsphere certificate of analysis data sheets provided by Bangs Laboratories, Inc.

Appendix B contains a description of preliminary studies that were conducted to determine important parameters when working with microspheres. These studies include proper sampling technique, sample volume, reservoir mixing rate, and minimum flow rate.

Appendix C describes the mini-column experiments that were conducted prior to the column experiments described in the manuscript. These mini-columns were conducted to get a feel for microsphere breakthrough.

Appendix D contains the figures, data tables, and plots for the experiments described in the manuscript: pictures of laboratory setup for the SMZ preparation and column experiments, a picture of particle suspension described under characterization of SMZ and zeolite surface properties, batch experiment tabulated data, figures of tritium BTCs and tabulated data, and microsphere BTCs, tabulated data, and microsphere fluorescent pictures of the zeolite media from the column experiments.

Appendix E contains the electrophoretic mobility zeta potential data sheet.

APPENDIX A. FLOW CYTOMETER ANALYSIS OF *CRYPTOSPORIDIUM* AND *GIARDIA* SURROGATES

As described in the manuscript, microsphere concentrations were analyzed using flow cytometry (FC) (FACScan Analyzer, Becton Dickenson Immunocytometry Systems, San Jose, CA). The sample particles flow up a 50-µm diameter tube and are excited by an argon laser at a wavelength of 488 nm. Three detectors measure emission at 530, 585 and 650 nm. Fluorescence intensity is correlated to microsphere size since larger microspheres have more fluorescence imbedded in them than smaller microspheres. Each florescence event is counted which can then be correlated to the concentration of microspheres/mL, using a standard curve of log counts verses log dilution factor. Per manufacturer specifications, the original concentrations of the 5-µm and 10-µm microspheres were 3.561×10^8 and 1.589×10^7 microspheres/mL, respectively.

Sample solutions were placed in 5-mL Becton Dickison falcon tubes (Fisher Scientific, Denver, CO) and covered with parafilm. Prior to analysis, samples were sonicated for 30 s and shaken well. Each sample was run for 3 min to obtain count per minute of microspheres per milliliter of sample (cpm/mL). The FC was set on high flow, and the average flow rate for all samples was 0.1 mL/min. Periodically the flow rate was checked gravimetrically during sample analysis.

Non-fluorescent microspheres of similar size to the fluorescent microspheres, along with pathogen-free effluent solution from the columns, were analyzed as a backgrounds to ensure that non-important particles would not be detected as

Cryptosporidium and *Giardia* microspheres. The microspheres were detected mostly as singlets (individual microspheres) however doublets (two microspheres stuck together) were detected in high-concentration samples, despite sonication.

Appendix Table A-1 is a series of dilutions of the original microsphere concentrations to determine the detection limit of the FC. Due to high cost of microspheres it was important to determine the minimum concentration of microspheres needed for reasonable detection on the FC. An initial solution concentration of 10^6 microspheres/mL was made and from that consecutive dilutions of 1:10 were prepared and analyzed. Appendix Table A-1 shows that as concentration of microspheres/mL increases, coefficient of variance between samples analyzed decreases resulting in better accuracy. At a microsphere concentration of about 10^3 cpm/mL, reasonable detection is obtained with a coefficient of variantion of 0.10 and 0.19 between replicates for 5- and 10-µm microspheres, respectively. In order to reasonably detect effluent concentrations of one-hundredth the input solution, input concentrations of 10^5 cpm/mL were used for all experiments. Appendix Figure A-1 is a plot of log total counts vs log dilution factor for the data in Appendix Table A-1. Linear standard curves were fit through the data and were used to correlate cpm/mL of sample to concentration of microspheres/mL of sample.

Microsphere certificates of analysis from Bangs Laboratories, Inc. are also provided in this appendix following the plots and figures.

Appendix Table A-1. Flow cytometer detection limit for microspheres.

Dilution Factor (microspheres:water)		Total Count (cpm/mL)		Actual Concentration (microspheres/mL)		Statistics Between Total Counts		
5 µm	10µm	5 µm	10 µm	5 µm	10 µm		5 µm	10 µm
blank	blank	0	0	0	0	Mean	0	0
blank	blank	0	0	0	0	Standard Deviation	0	0
blank	blank	0	0	0	0	Coefficient of Variation	0.00	0.00
$1{:}10^6$	$1{:}10^5$	68	63	3.6×10^2	1.6×10^2	Mean	69	50
$1{:}10^6$	$1{:}10^5$	84	67	3.6×10^2	1.6×10^2	Standard Deviation	16	26
$1{:}10^6$	$1{:}10^5$	53	20	3.6×10^2	1.6×10^2	Coefficient of Variation	0.23	0.52
$1{:}10^5$	$1{:}10^4$	1022	1030	3.6×10^3	1.6×10^3	Mean	918	884
$1{:}10^5$	$1{:}10^4$	891	923	3.6×10^3	1.6×10^3	Standard Deviation	94	168
$1{:}10^5$	$1{:}10^4$	841	700	3.6×10^3	1.6×10^3	Coefficient of Variation	**0.10**	**0.19**
$1{:}10^4$	$1{:}10^3$	15050	14763	3.6×10^4	1.6×10^4	Mean	14369	13706
$1{:}10^4$	$1{:}10^3$	13926	12517	3.6×10^4	1.6×10^4	Standard Deviation	599	1129
$1{:}10^4$	$1{:}10^3$	14132	13837	3.6×10^4	1.6×10^4	Coefficient of Variation	0.04	0.08
$1{:}10^3$	$1{:}10^2$	124474	113177	3.6×10^5	1.6×10^5	Mean	124474	113177

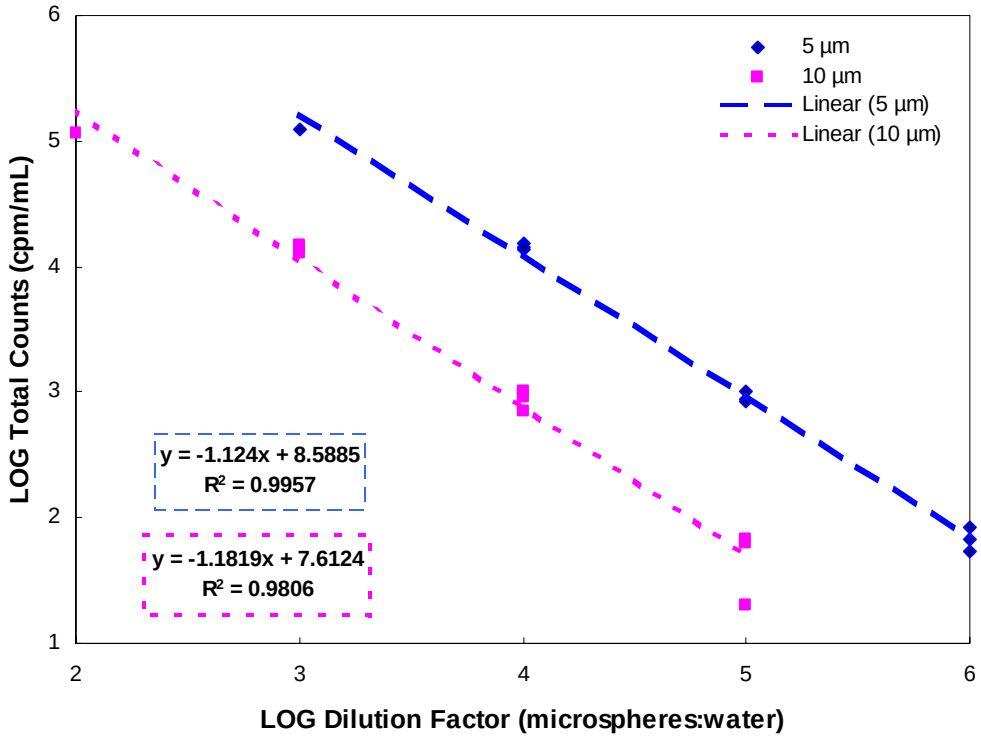

Appendix Figure A-1. Flow cytometer standard curve.

9025 Technology Dr. • Fishers, IN 46038-2886
800.387.0672 o 317.570.7020 o Fax 317.570.7034
email:info@bangslabs.com o www.bangslabs.com

Bangs Laboratories, Inc.

BEADS • ABOVE THE REST

CERTIFICATE OF ANALYSIS

Particle Description

Catalog Code: **FC06F** Manufacturer Lot Number: **6456** Inventory Number: **L040129H** Product Class: **Standard**

Polymer Description: **P(S/7%DVB/5%MAA)•(480,520)**

Characteristics

Surface Functional Groups:	**COOH/1**	Color:	**Dragon Green**
Solids Content (wt. %):	**1**	Standard Deviation #1 (μm):	**0.14**
Antimicrobial:	**2mM NaN3**	Microbial Load:	**No growth 2/5/04**
Surface Titration Data (μeq/g):	**4.1**	Binding Capacity:	**0**
Mean Diameter #1 (μm):	**5.01 (Coulter Principle)**		
Buffer:	**DI water + 0.01% Tween 20**		

Calculated Data

Density of Solid Polymer¥ (g/ml):	**1.1**	Parking Area ($Å^2$/ Surface Group):	**44.5**
Number of Microspheres/gram*:	**1.381e+10**	Number of Microspheres per ml:	**1.382e+8**
Surface area ($μm^2$/g):	**1.089e+12**		

Approved by Quality Department Date of issue: **February 5, 2004**

Recommended Storage Conditions:
Aqueous microspheres should be stored at 2-8°C. AVOID FREEZING!
Dry microspheres do not require special storage conditions.
Magnetic materials should be stored at 2-8°C while being rotated at slow speed to keep the microspheres from settling.
ProActive™ material (protein coated) should be stored at 2-8°C.

¥Density of bulk polymer: a 1 cm cube of Polystrene weighs 1.05g
*Number of particles per gram of dry particles.

In an effort to save trees we do not routinely send Material Safety Data Sheets with our shipments. However, if you would like to receive one please call Customer Service at 800-387-0672 or 317-570-7020.

9025 Technology Dr. • Fishers, IN 46038-2886
800.387.0672 o 317.570.7020 o Fax 317.570.7034
email:info@bangslabs.com o www.bangslabs.com

Bangs Laboratories, Inc.

BEADS • ABOVE THE REST

CERTIFICATE OF ANALYSIS

Particle Description

Catalog Code: **FC07F** Manufacturer Lot Number: **4772** Inventory Number: **L001012C** Product Class: **Standard**

Polymer Description: **P(S/V-COOH)•(480,520)**

Characteristics

Surface Functional Groups:	**COOH/1**	Color:	**Dragon Green**
Solids Content (wt. %):	**1**	Standard Deviation #1 (µm):	**1.09**
Antimicrobial:	**2 mM Sodium Azide**	Surface Titration Data (µeq/g):	**5.0**
Binding Capacity:	**0**		
Mean Diameter #1 (µm):	**10.43 (Coulter Principle)**		
Buffer:	**DI water + 0.1% Tween**		

Calculated Data

Density of Solid Polymer¥ (g/ml):	**1.06**	Parking Area ($Å^2$/ Surface Group):	**18**
Number of Microspheres/gram*:	**1.588e+9**	Number of Microspheres per ml:	**1.589e+7**
Surface area ($µm^2$/g):	**5.427e+11**		

Approved by Quality Department Date of issue: **February 5, 2004**

Recommended Storage Conditions:
Aqueous microspheres should be stored at 2-8°C. AVOID FREEZING!
Dry microspheres do not require special storage conditions.
Magnetic materials should be stored at 2-8°C while being rotated at slow speed to keep the microspheres from settling.
ProActive™ material (protein coated) should be stored at 2-8°C.

¥Density of bulk polymer: a 1 cm cube of Polystrene weighs 1.05g
*Number of particles per gram of dry particles.

In an effort to save trees we do not routinely send Material Safety Data Sheets with our shipments. However, if you would like to receive one please call Customer Service at 800-387-0672 or 317-570-7020.

APPENDIX B. PRELIMINARY STUDIES

Preliminary studies were conducted to investigate experiment parameters. These studies include proper sampling technique, sample volume, reservoir mixing rate, and minimum flow rate.

Sampling technique was analyzed and data is tabulated in Appendix Table B-1. Five 4-mL samples were collected using the same glass pipet and five 4-mL samples were collected using different pipets for each. For all samples each pipet was rinsed with stock solution once before the sample(s) were collected. When the same pipet was used to collect all five samples there was a 0.05 and 0.02 coefficient of variation among 5 and 10-μm microsphere concentrations, respectively. When a different pipet was used to collect each sample there was a 0.01 and 0.02 coefficient of variation among 5- and 10-μm microsphere concentrations, respectively. There may be slight microsphere interaction when using the same pipet for multiple samples, however, the variability between sampling with the same pipet verses a different pipet is not significant to draw conclusions.

Analysis was conducted to determine if sample volume contributes to reproducibility of microsphere concentrations. To test this, the same procedures were conducted as above for testing sample technique, however, a 2mL volume was collected for each sample. Data is tabulated in Appendix Table B-2 and compared to data in Appendix Table B-1. Sample volumes of 2 mL give a larger coefficient of variation among replicates. For samples collected with the same pipet, coefficient of variation was 0.37 and 0.08 for 5- and 10-μm microspheres, respectively; and for sample collected with

a different pipet, coefficient of variation was 0.15 and 0.18 for 5-µm and 10-µm microspheres, respectively. Again, there may be microsphere interaction with the glass pipet, with a more pronounced effect for smaller sample volumes. Thus, 4-mL sample volumes were collected for all experiments to reduce the amount of variability in the data due to microsphere surface interactions.

Due to their large size, the microspheres are subject to settling within the reservoir and feed lines before entering the filtration media. Thus, studies were conducted to determine the appropriate mixing rate of the reservoir. Data is tabulated in Appendix Table B-3. To test settling in the reservoir, the stock solution was well mixed and placed on a stirrer at 100 rpm. Three initial samples were collected and then after 4.5 h of stirring, three samples were collected at the top middle and bottom of the reservoir. The coefficient of variation between all sample collected was 0.04 and 0.06 for 5- and 10-µm microspheres, respectively. After 4.5 h there was no significant indication of settling in the reservoir. To ensure that no settling would occur over longer periods of time, the stock solution was mixed at about 300 rpm for the duration of all experiments.

Next, studies were conducted to test the minimum flow rate through the system in order to prevent microspheres from settling within the feed lines, Appendix Table B-4 and Appendix Figure B-1. Five different flow rates were tested ranging from 0.125 to 0.5 mL/min. For each test, the feed lines were purged with fresh stock solution and the microsphere concentration was sampled at 0-PV through the inlet stopcock of the column. Then, after 5-PV of stock solution had flowed through the feed lines the microsphere concentration was again sampled at the inlet stopcock. The percent change in 0 to 5-PV was calculated for each flow rate. The percent change ranged from 7-22%

and 6-58% for the 5- and 10-µm microspheres, respectively, with the larger percent change corresponding to the lowest flow rate. It was also observed that flow rates through the column greater than 1.0 mL/min would dislodge SMZ particles and cause a murky effluent. Thus, to ensure that there was minimal settling of microspheres within the feed lines and that SMZ particles would not be dislodged, the minimum flow rate used for all experiments was 0.9 mL/min.

Appendix Table B-1. Sample technique (4.0 mL sample volume).

Sample ID_#	Total Counts (cpm/mL)		Concentration (microspheres/mL)		Statistics for Each Sample Technique		
	5 µm	10 µm	5 µm	10 µm		5 µm	10 µm
Same Pipet_1	10503	12687	30779	17066	**Average**	30387	17616
Same Pipet_2	9443	13157	27999	17599	**Standard Deviation**	1514	409
Same Pipet_3	10973	12973	32001	17392	**Coefficient of Variance**	**0.05**	**0.02**
Same Pipet_4	10210	13483	30013	17968			
Same Pipet_5	10643	13560	31143	18055			
Different Pipet_1	10947	13417	31932	17893	**Average**	32053	17693
Different Pipet_2	11160	12987	32485	17407	**Standard Deviation**	266	279
Different Pipet_3	10987	13203	32036	17652	**Coefficient of Variance**	**0.01**	**0.02**
Different Pipet_4	10990	13030	32044	17456			
Different Pipet_5	10883	13560	31767	18055			

Appendix Table B-2. Sample technique (2.0 mL sample volume).

Sample ID_#	Total Counts (cpm/mL)		Concentration (microspheres/mL)		Statistics for Each Sample Technique		
	5 µm	10 µm	5 µm	10 µm		5 µm	10 µm
Same Pipet_1	8463	10110	25399	14083	**Average**	23452	15434
Same Pipet_2	6163	10590	19155	14647	**Standard Deviation**	8793	1227
Same Pipet_3	10417	11560	30553	15775	**Coefficient of Variance**	**0.37**	**0.08**
Same Pipet_4	3123	11213	10463	15373			
Same Pipet_5	10853	12887	31690	17293			
Different Pipet_1	6063	7660	18878	11136	**Average**	27153	15204
Different Pipet_2	9940	12150	29306	16453	**Standard Deviation**	4856	2279
Different Pipet_3	10503	11853	30779	16113	**Coefficient of Variance**	**0.18**	**0.15**
Different Pipet_4	10197	11997	29978	16277			
Different Pipet_5	9000	11790	26827	16040			

Appendix Table B-3. Reservoir mixing rate (all samples taken at 100 rpm).

Sample ID_#	Total Counts (cpm/mL)		Concentration (microspheres/mL)		Statistics for All Samples		
	5 µm	10 µm	5 µm	10 µm		5 µm	10 µm
Initial_1	11887	11983	34360	16262	**Average**	31962	15808
Initial_2	11197	11820	32580	16074	**Standard Deviation**	1866	638
Initial_3	11513	12280	33398	16602	**Coefficient of Variance**	**0.06**	**0.04**
Top_1	10470	10690	30692	14764			
Top_2	11833	12140	34223	16442			
Top_3	11700	12203	33880	16514			
Middle_1	10697	11330	31282	15509			
Middle_2	10810	11667	31577	15898			
Middle_3	11190	10603	32563	14663			
Bottom_1	10357	11263	30396	15431			
Bottom_2	9547	11470	28272	15671			
Bottom_3	10330	11643	30326	15871			

Appendix Table B-4. Minimum flow rate through system.

Flow Rate_Pore Volume (mL/min)_(mL)	Total Counts (cpm/mL)		Concentration (microspheres/mL)		% Change	
	5 µm	10 µm	5 µm	10 µm	5 µm	10 µm
0.5_0	7769	3551	23536	5811		
0.5_5	8343	3821	25078	6183	**7**	**6**
0.45_0	6214	4292	19296	6822		
0.45_5	7466	3134	22717	5229	18	23
0.35_0	7838	3459	23722	5683		
0.35_5	5434	2406	17126	4180	28	26
0.25_0	9941	3890	29309	6277		
0.25_5	7816	2548	23662	4388	19	30
0.125_0	6799	1621	20903	2993		
0.125_5	5106	582	16200	1258	22	58

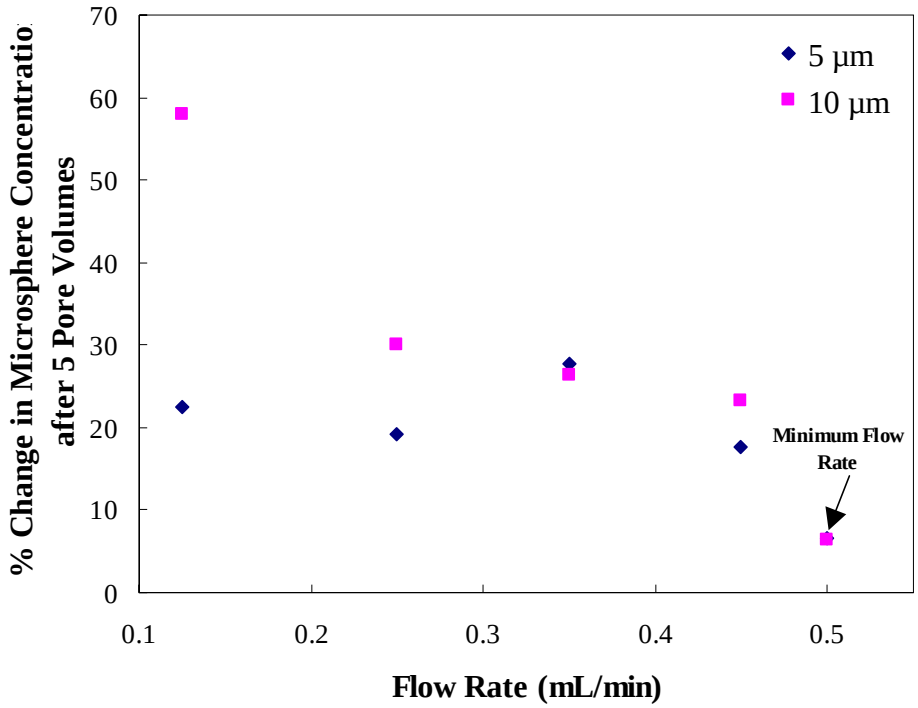

Appendix Figure B-1. Minimum flow rate through system.

APPENDIX C. MINI-COLUMN EXPERIMENTS

Prior to the column experiments described in the manuscript, rapid mini-column experiments were conducted to get a feel for microsphere breakthrough on the cationic SMZ, hydrophobic SMZ, and zeolite, as well as, the aquifer sand medium.

Mini-columns were constructed from Teflon tubing with a 1.0-cm inner diameter and 5-cm length. Nylon screen (30 μm) was used to retain the filter media within the column and three-way check valves (Cole-Palmer, Vernon Hills, IL) were connected to the ends. These valves serve as sample ports and sealed the columns shut between experiments. Using a total of four columns the cationic SMZ, hydrophobic SMZ, zeolite all 1.4-2.4 mm and aquifer sand 0.18 mm-0.71 mm were packed into the columns, saturated, and the PVs determined as described in the manuscript. Twenty PVs of stock solution (10^5 microspheres/mL) was continuously injected into the columns at a flow rate of 0.9 mL/min and 4-mL samples were collected continuously in falcon analysis tubes while the input concentration was sampled periodically throughout the experiment.

Microsphere concentrations were analyzed as described in the manuscript and data is tabulated in Appendix Table C-1. Breakthrough curves of microspheres for each material are plotted in Appendix Figures C-1 through C-4. Removal efficiencies were calculated as described in the manuscript and are listed in Appendix Table C-2. All four mini-columns yielded actual removal efficiencies in the range of 20 to 96% for the 5-μm microspheres and 65 to 100% for the 10-μm microspheres. Sand has a much smaller grain size than the SMZ and zeolite materials and proved to be the most efficient at removing

microspheres from solution. Among the similar sized materials the cationic SMZ adsorbed the most microspheres followed by the hydrophobic SMZ and the least efficient, zeolite.

The data obtained in the mini-column experiments cannot be directly compared to the larger column experiment data described in the manuscript. The mini-column and larger column experiments differ in terms of linear velocity through each column. The mini-columns had faster linear velocities ranging from 2.40 to 3.91 cm/min. The larger columns had a slower linear velocities ranging from 0.25 to 0.29 cm/min. Tritium tracer tests were not conducted through the mini-columns, however should channeling have existed, these effects would be amplified for the smaller volume mini-columns.

Appendix Table C-1. Breakthrough data for all mini-columns.

	Cationic SMZ			Hydrophobic SMZ			Zeolite			Sand		
Sample	**PV**	**5 µm C/Co**	**10 µm C/Co**	**PV**	**5 µm C/Co**	**10 µm C/Co**	**PV**	**5 µm C/Co**	**10 µm C/Co**	**PV**	**5 µm C/Co**	**10 µm C/Co**
1	0.4	0.08	0.03	0.3	0.12	0.06	0.3	0.07	0.04	0.8	0.01	0.00
2	1.1	0.18	0.05	1.0	0.36	0.20	0.9	0.44	0.31	1.4	0.01	0.00
3	1.9	0.21	0.08	1.7	0.39	0.26	1.7	0.73	0.36	2.4	0.03	0.00
4	2.6	0.23	0.08	2.4	0.45	0.29	2.4	0.84	0.29	3.5	0.05	0.00
5	3.4	0.24	0.08	3.1	0.47	0.30	3.0	0.78	0.32	4.6	0.04	0.00
6	4.2	0.27	0.11	3.9	0.46	0.24	3.7	0.82	0.47	5.8	0.06	0.00
7	5.0	0.26	0.09	4.6	0.42	0.24	4.3	0.71	0.29	6.9	0.04	0.00
8	5.8	0.38	0.16	5.3	0.59	0.40	5.0	0.76	0.29	8.1	0.04	0.00
9	6.5	0.41	0.16	6.0	0.56	0.34	5.8	0.79	0.29	9.3	0.04	0.00
10	7.4	0.31	0.09	6.8	0.44	0.24	6.5	0.79	0.31	10.6	0.05	0.00
11	8.1	0.28	0.07	7.5	0.46	0.22	7.2	0.92	0.38	11.8	0.05	0.00
12	8.9	0.28	0.08	8.2	0.46	0.22	8.0	0.79	0.28	13.1	0.04	0.00
13	9.7	0.29	0.10	9.0	0.50	0.29	8.7	0.88	0.37	14.4	0.04	0.00
14	10.5	0.31	0.11	9.7	0.50	0.30	9.4	0.85	0.35	15.7	0.04	0.00
15	11.3	0.30	0.12	10.4	0.57	0.31	10.1	0.84	0.35	16.9	0.04	0.00
16	12.1	0.36	0.13	11.2	0.53	0.27	10.8	0.88	0.39	18.2	0.06	0.00
17	12.9	0.34	0.11	11.9	0.50	0.23	11.6	0.79	0.34	19.4	0.05	0.00
18	13.7	0.32	0.12	12.7	0.57	0.29	12.3	0.86	0.46	20.6	0.04	0.00
19	14.5	0.35	0.13	13.4	0.56	0.27	13.1	0.86	0.43	21.9	0.05	0.00
20	15.4	0.33	0.13	14.2	0.58	0.30	13.9	0.84	0.44	23.2	0.04	0.00

Appendix Table C-2. Removal efficiencies of microspheres for all mini-columns.

	(%)	
	5 µm	**10 µm**
Cationic SMZ	70	89
Hydrophobic SMZ	51	73
Zeolite	20	65
Sand	96	100

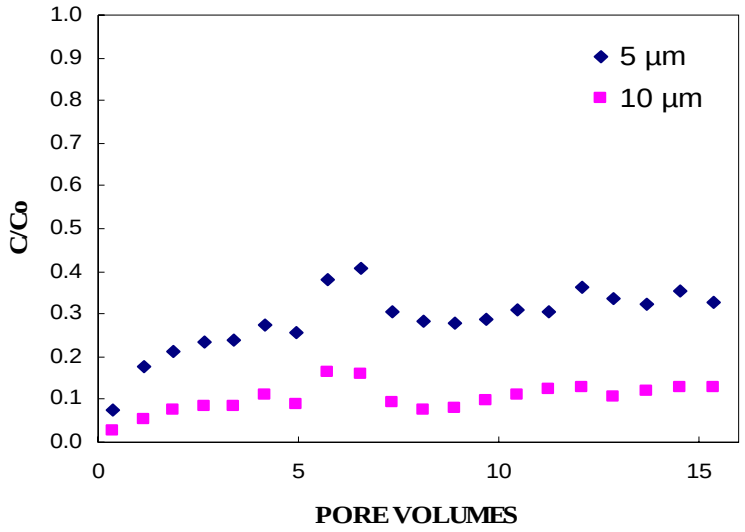

Appendix Figure C-1. **Mini-column experiment microsphere BTC for cationic SMZ.**

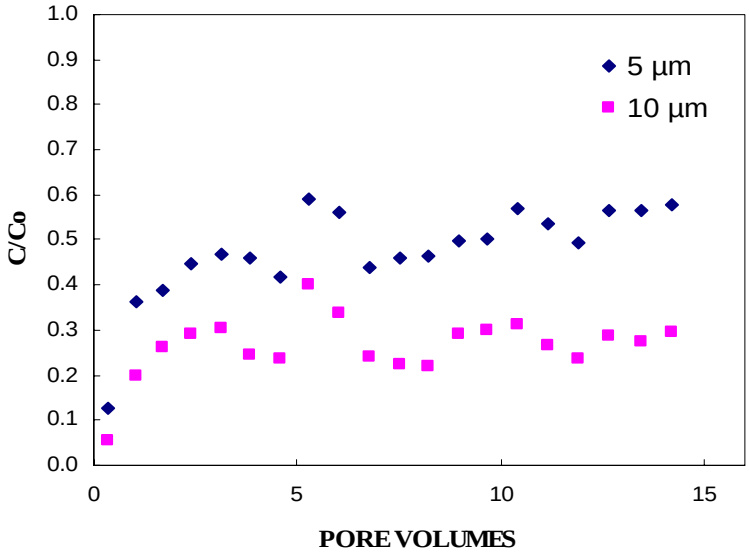

Appendix Figure C-2. **Mini-column experiment microsphere BTC for hydrophobic SMZ.**

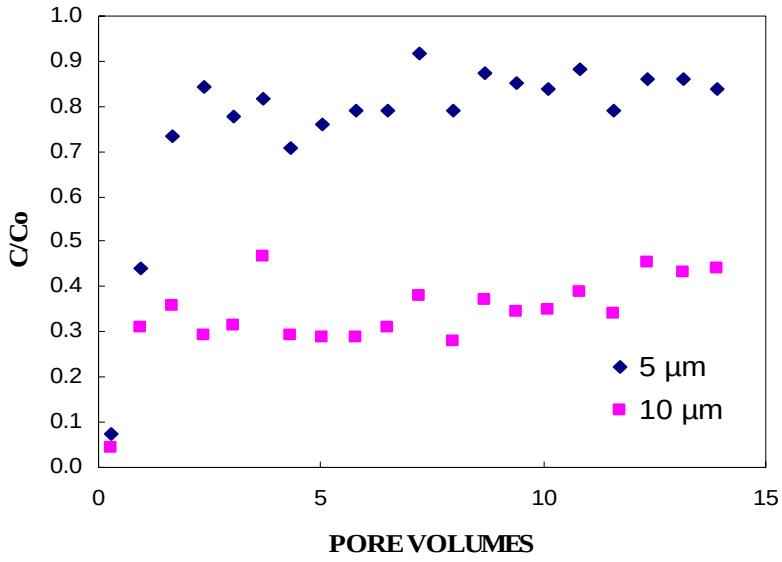

Appendix Figure C-3. Mini-column experiment microsphere BTC for zeolite.

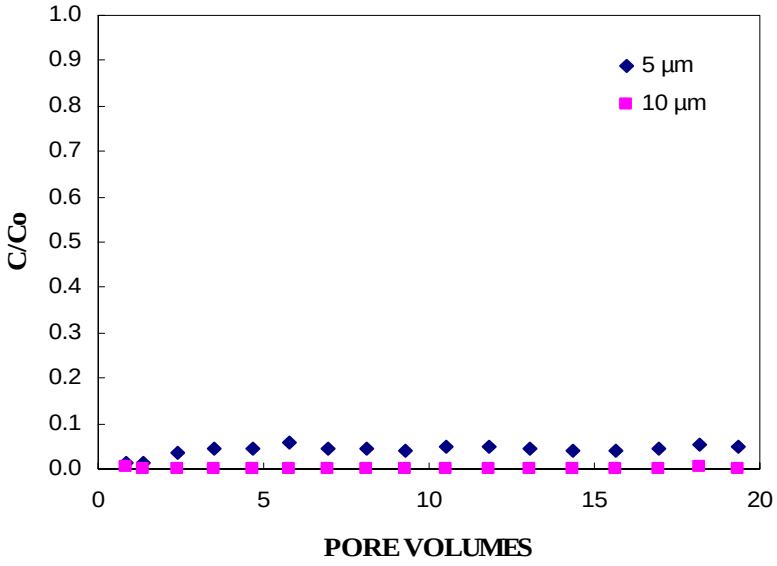

Appendix Figure C-4. Mini-column experiment microsphere BTC for sand.

APPENDIX D. DATA TABLES AND PLOTS FOR EXPERIMENTS DESCRIBED IN THE MANUSCRIPT

Laboratory setup for the SMZ preparation and the column experiments described in the manuscript are illustrated in Appendix Figures D-1 and D-2. As described in the manuscript under characterization of SMZ and zeolite surface properties Appendix Figure D-3 shows a visual of particle suspension observed for the cationic SMZ (CSMZ), hydrophobic SMZ (HSMZ), and zeolite in DI water mixtures.

Figures 2 and 3 of the manuscript show the batch experiment data plotted as *S* vs *Ce* with a linear fit through zero. The tabulated data for those plots is presented in Appendix Table D-1 and D-2, which list *S* and *Ce* values determined for the cationic SMZ, hydrophobic SMZ, zeolite, and sand with varying *Co* microsphere concentrations.

Appendix Figures D-4 through D-8 are plots of the observed and fitted tritium BTC data for the Cationic SMZ 2, Hydrophobic SMZ 1, Hydrophobic SMZ 2, Zeolite 1, and Zeolite 2 column tracer tests. The plot for Cationic SMZ 1 is shown in Figure 4 of the manuscript. The tabulated data for these plots is listed in Appendix Table D-3.

The observed microsphere BTC of the column experiments are shown in Appendix Figures D-9 and D-10 for Cationic SMZ 2, Hydrophobic SMZ 2, and Zeolite 2. The microsphere BTC for Cationic SMZ 1, Hydrophobic SMZ 1, and Zeolite 1 are shown in Figures 5 and 6 of the manuscript. The tabulated data for these plots are listed in Appendix Table D-4.

As described in the manuscript, pictures of the material and sorbed microspheres removed from columns Zeolite 1 and Zeolite 2 for visually inspected under ultraviolet

light are presented in Appendix Figure D-11 with notation (1a)-(1e) for Zeolite 1 and (2a)-(2e) for Zeolite 2, (a) through (e) corresponding to the sections taken from the bottom (1a) and (2a), near the inlet, up the column length. These pictures must be viewed with color to see the microsphere fluorescence (green) within each section. The most intense fluorescence is seen in sections (a) for each with some in sections (b). There is no fluorescence visible in sections (c) through (e) for either column.

Appendix Figure D-1. Laboratory setup for SMZ preparation.

Appendix Figure D-2. Laboratory setup for column experiments.

Appendix Figure D-3. **Particle suspension observed for cationic SMZ (CSMZ), hydrophobic SMZ (HSMZ), and zeolite in DI water.**

Appendix Table D-1. Batch experiment data for 5-µm microspheres.

	Co **(microspheres/mL)**	***Ce*** **(microspheres/mL)**	***S*** **(microspheres/g)**
Cationic SMZ 1	1237	5	2464
Cationic SMZ 2	1237	0	2474
Cationic SMZ 1	5135	6	10258
Cationic SMZ 2	5135	11	10248
Cationic SMZ 1	51542	44	102996
Cationic SMZ 2	51542	55	102974
Hydrophobic SMZ 1	1237	0	2474
Hydrophobic SMZ 2	1237	0	2474
Hydrophobic SMZ 1	5135	9	10252
Hydrophobic SMZ 2	5135	4	10262
Hydrophobic SMZ 1	51542	96	102892
Hydrophobic SMZ 2	51542	38	103008
Zeolite 1	1237	12	2450
Zeolite 2	1237	14	2446
Zeolite 1	5135	100	10070
Zeolite 2	5135	109	10052
Zeolite 1	51542	736	101612
Zeolite 2	51542	737	101610
Sand 1	1237	17	2440
Sand 2	1237	21	2432
Sand 1	5135	129	10012
Sand 2	5135	136	9998
Sand 1	51542	982	101120
Sand 2	51542	952	101180

Appendix Table D-2. Batch experiment data for 10-µm microspheres.

	Co **(microspheres/mL)**	***Ce*** **(microspheres/mL)**	***S*** **(microspheres/g)**
Cationic SMZ 1	1453	149	2608
Cationic SMZ 2	1453	291	2324
Cationic SMZ 1	4498	459	8077
Cationic SMZ 2	4498	588	7819
Cationic SMZ 1	36397	3219	66355
Cationic SMZ 2	36397	3656	65481
Hydrophobic SMZ 1	1453	73	2760
Hydrophobic SMZ 2	1453	121	2664
Hydrophobic SMZ 1	4498	481	8033
Hydrophobic SMZ 2	4498	159	8677
Hydrophobic SMZ 1	36397	3280	66233
Hydrophobic SMZ 2	36397	1831	69131
Zeolite 1	1453	384	2138
Zeolite 2	1453	384	2138
Zeolite 1	4498	2017	4961
Zeolite 2	4498	2089	4817
Zeolite 1	36397	12177	48439
Zeolite 2	36397	13135	46523
Sand 1	1453	414	2078
Sand 2	1453	609	1688
Sand 1	4498	2515	3965
Sand 2	4498	2776	3443
Sand 1	36397	18803	35187
Sand 2	36397	17905	36983

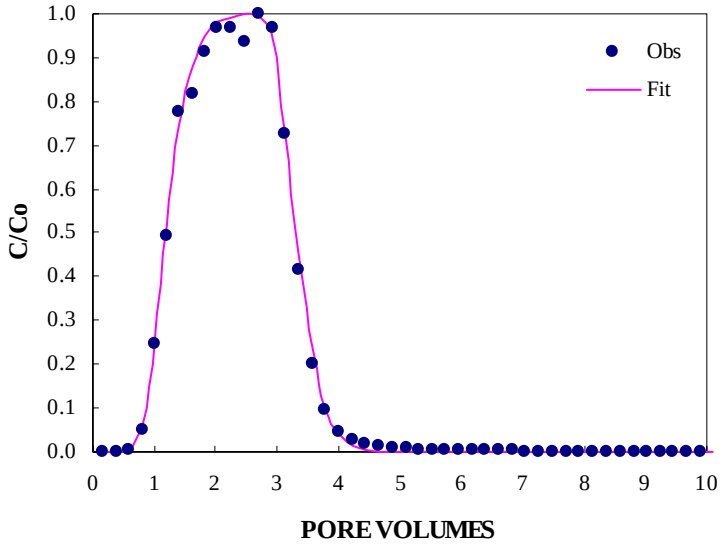

Appendix Figure D-4. **Observed and fitted (Eq. 2) BTC for tritiated water in column Cationic SMZ 2.**

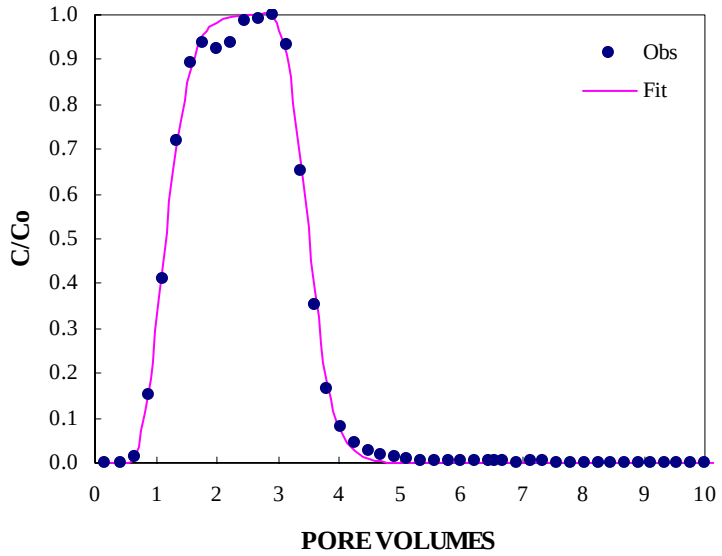

Appendix Figure D-5. **Observed and fitted (Eq. 2) BTC for tritiated water in column Hydrophobic SMZ 1.**

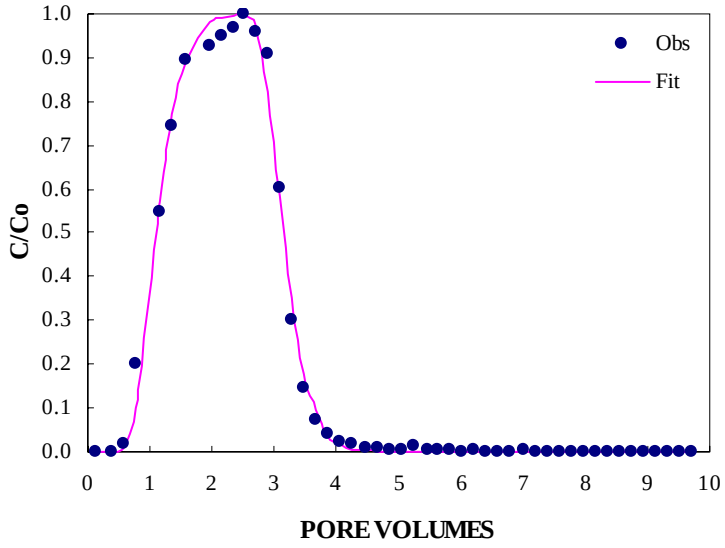

Appendix Figure D-6. **Observed and fitted (Eq. 2) BTC for tritiated water in column Hydrophobic SMZ 2.**

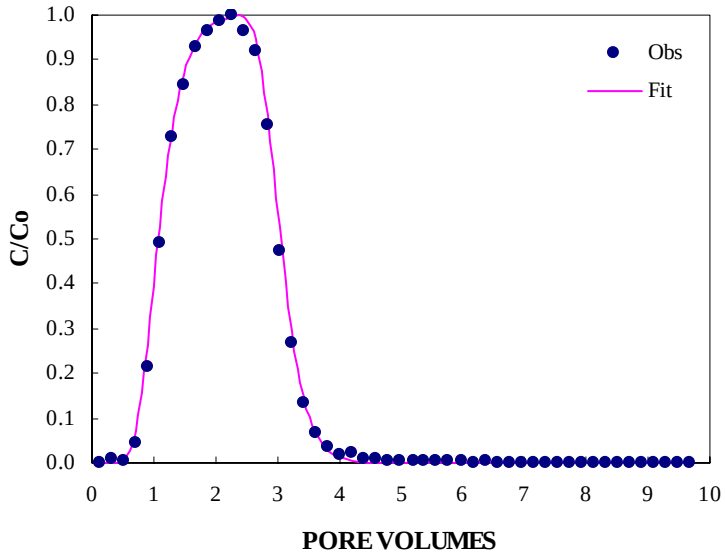

Appendix Figure D-7. **Observed and fitted (Eq. 2) BTC for tritiated water in column Zeolite 1.**

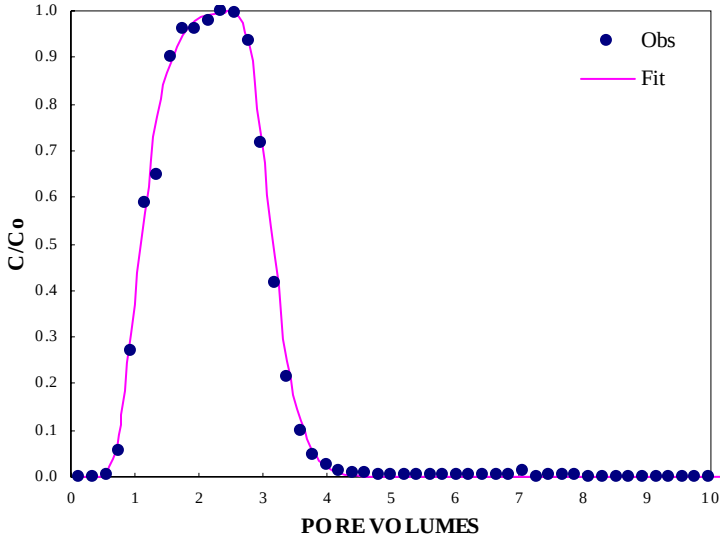

Appendix Figure D-8. **Observed and fitted (Eq. 2) BTC for tritiated water in column Zeolite 2.**

Appendix Table D-3. Tritium observed and fitted (Eq. 2) BTC data for all columns.

Cationic SMZ 1			Cationic SMZ 2			Hydrophobic SMZ 1			Hydrophobic SMZ 2			Zeolite 1			Zeolite 2		
	Obs.	Fit		Obs.	Fit		Obs.	Fit		Obs.	Fit		Obs.	Fit		Obs.	Fit
PV	C/Co	C/Co	PV	C/Co	C/Co	PV	C/Co	C/Co	PV	C/Co	C/Co	PV	C/Co	C/Co	PV	C/Co	C/Co
0.065	0.002	0.000	0.147	0.002	0.000	0.157	0.002	0.000	0.139	0.002	0.000	0.115	0.002	0.000	0.121	0.002	0.000
0.228	0.002	0.000	0.396	0.002	0.000	0.428	0.002	0.000	0.378	0.002	0.000	0.330	0.009	0.000	0.344	0.001	0.000
0.421	0.002	0.000	0.598	0.003	0.004	0.653	0.012	0.015	0.577	0.016	0.010	0.524	0.004	0.004	0.547	0.004	0.007
0.613	0.007	0.009	0.798	0.049	0.066	0.876	0.150	0.160	0.772	0.201	0.099	0.715	0.044	0.070	0.747	0.058	0.089
0.806	0.083	0.103	0.999	0.245	0.257	1.101	0.411	0.441	1.163	0.550	0.570	0.909	0.212	0.262	0.949	0.270	0.306
1.002	0.298	0.320	1.203	0.494	0.517	1.328	0.718	0.714	1.364	0.745	0.770	1.106	0.492	0.526	1.155	0.589	0.565
1.200	0.565	0.585	1.411	0.779	0.743	1.558	0.891	0.879	1.561	0.897	0.890	1.299	0.726	0.733	1.357	0.647	0.774
1.394	0.792	0.778	1.617	0.818	0.882	1.785	0.939	0.955	1.956	0.926	0.980	1.490	0.846	0.865	1.555	0.903	0.887
1.587	0.900	0.898	1.820	0.915	0.948	2.010	0.922	0.984	2.158	0.950	0.992	1.682	0.928	0.937	1.754	0.963	0.950
1.783	0.934	0.955	2.027	0.966	0.980	2.238	0.937	0.995	2.341	0.968	0.997	1.872	0.966	0.972	1.952	0.962	0.979
1.992	0.967	0.983	2.248	0.969	0.993	2.470	0.987	0.998	2.521	1.000	0.998	2.063	0.989	0.988	2.151	0.978	0.992
2.205	1.000	0.994	2.476	0.934	0.998	2.702	0.991	1.000	2.714	0.959	0.971	2.259	1.000	0.996	2.358	1.000	0.997
2.615	0.970	0.951	2.697	1.000	0.997	2.927	1.000	0.995	2.907	0.908	0.824	2.459	0.962	0.996	2.565	0.994	0.995
2.820	0.710	0.758	2.916	0.968	0.940	3.150	0.932	0.913	3.098	0.604	0.584	2.656	0.920	0.948	2.770	0.934	0.932
3.231	0.230	0.256	3.138	0.724	0.730	3.372	0.651	0.668	3.291	0.301	0.351	2.848	0.755	0.775	2.971	0.718	0.733
3.442	0.108	0.115	3.355	0.416	0.446	3.591	0.351	0.382	3.488	0.146	0.179	3.042	0.473	0.526	3.172	0.416	0.472
3.651	0.056	0.047	3.574	0.201	0.232	3.814	0.165	0.180	3.681	0.072	0.096	3.239	0.268	0.295	3.376	0.214	0.251
3.860	0.027	0.018	3.795	0.095	0.101	4.040	0.082	0.071	3.872	0.040	0.039	3.437	0.135	0.146	3.583	0.099	0.122
4.068	0.020	0.006	4.014	0.047	0.040	4.262	0.044	0.026	4.063	0.024	0.017	3.632	0.065	0.068	3.785	0.047	0.052
4.278	0.013	0.002	4.230	0.028	0.014	4.478	0.026	0.009	4.260	0.016	0.007	3.826	0.035	0.029	3.986	0.025	0.022
4.488	0.010	0.001	4.445	0.019	0.005	4.692	0.016	0.003	4.461	0.011	0.003	4.021	0.019	0.012	4.192	0.015	0.009
4.696	0.009	0.000	4.665	0.013	0.002	4.910	0.012	0.001	4.660	0.008	0.001	4.219	0.020	0.005	4.399	0.010	0.003
4.904	0.005	0.000	4.886	0.010	0.001	5.130	0.009	0.000	4.856	0.006	0.000	4.415	0.008	0.002	4.601	0.007	0.001
5.112	0.006	0.000	5.101	0.008	0.000	5.348	0.006	0.000	5.053	0.005	0.000	4.609	0.007	0.001	4.801	0.006	0.001
5.320	0.005	0.000	5.313	0.006	0.000	5.566	0.005	0.000	5.254	0.012	0.000	4.802	0.006	0.000	5.003	0.005	0.000
5.526	0.005	0.000	5.529	0.005	0.000	5.787	0.004	0.000	5.452	0.003	0.000	4.999	0.005	0.000	5.207	0.004	0.000
5.729	0.004	0.000	5.747	0.005	0.000	6.013	0.003	0.000	5.642	0.003	0.000	5.195	0.004	0.000	5.413	0.004	0.000
5.934	0.004	0.000	5.962	0.004	0.000	6.238	0.004	0.000	5.833	0.003	0.000	5.388	0.004	0.000	5.615	0.003	0.000
6.143	0.003	0.000	6.176	0.003	0.000	6.458	0.003	0.000	6.026	0.002	0.000	5.580	0.003	0.000	5.815	0.004	0.000
6.353	0.003	0.000	6.389	0.003	0.000	6.571	0.003	0.000	6.221	0.002	0.000	5.775	0.003	0.000	6.018	0.003	0.000
6.559	0.004	0.000	6.611	0.003	0.000	6.689	0.003	0.000	6.414	0.002	0.000	5.972	0.003	0.000	6.227	0.003	0.000
6.762	0.003	0.000	6.833	0.003	0.000	6.916	0.002	0.000	6.605	0.002	0.000	6.168	0.002	0.000	6.436	0.003	0.000
6.969	0.003	0.000	7.050	0.002	0.000	7.138	0.002	0.000	6.799	0.001	0.000	6.361	0.002	0.000	6.642	0.003	0.000
7.176	0.003	0.000	7.266	0.002	0.000	7.356	0.002	0.000	6.997	0.002	0.000	6.554	0.001	0.000	6.848	0.003	0.000
7.381	0.003	0.000	7.484	0.002	0.000	7.578	0.002	0.000	7.193	0.002	0.000	6.750	0.002	0.000	7.059	0.013	0.000
7.584	0.002	0.000	7.704	0.002	0.000	7.804	0.002	0.000	7.384	0.002	0.000	6.947	0.002	0.000	7.269	0.002	0.000
7.789	0.002	0.000	7.927	0.002	0.000	8.029	0.002	0.000	7.576	0.002	0.000	7.142	0.002	0.000	7.477	0.002	0.000
7.998	0.003	0.000	8.147	0.002	0.000	8.250	0.002	0.000	7.769	0.002	0.000	7.334	0.002	0.000	7.682	0.002	0.000
8.207	0.002	0.000	8.366	0.002	0.000	8.471	0.002	0.000	7.965	0.002	0.000	7.530	0.002	0.000	7.891	0.002	0.000
8.413	0.002	0.000	8.590	0.002	0.000	8.693	0.002	0.000	8.160	0.002	0.000	7.728	0.002	0.000	8.102	0.002	0.000
8.615	0.002	0.000	8.815	0.002	0.000	8.912	0.002	0.000	8.351	0.002	0.000	7.923	0.002	0.000	8.310	0.002	0.000
8.817	0.002	0.000	9.036	0.002	0.000	9.129	0.002	0.000	8.545	0.002	0.000	8.116	0.002	0.000	8.516	0.002	0.000
9.022	0.002	0.000	9.249	0.002	0.000	9.342	0.002	0.000	8.742	0.002	0.000	8.309	0.002	0.000	8.725	0.002	0.000
9.225	0.002	0.000	9.461	0.002	0.000	9.554	0.002	0.000	8.936	0.002	0.000	8.507	0.002	0.000	8.935	0.002	0.000
9.426	0.002	0.000	9.676	0.002	0.000	9.770	0.002	0.000	9.128	0.002	0.000	8.706	0.002	0.000	9.145	0.002	0.000
9.628	0.004	0.000	9.889	0.002	0.000	9.987	0.002	0.000	9.320	0.002	0.000	8.902	0.002	0.000	9.353	0.001	0.000
9.834	0.002	0.000	10.099	0.002	0.000	10.200	0.002	0.000	9.514	0.002	0.000	9.096	0.002	0.000	9.557	0.002	0.000
10.054	0.002	0.000							9.724	0.002	0.000	9.293	0.002	0.000	9.762	0.002	0.000
												9.493	0.002	0.000	9.969	0.002	0.000
												9.689	0.002	0.000	10.173	0.002	0.000

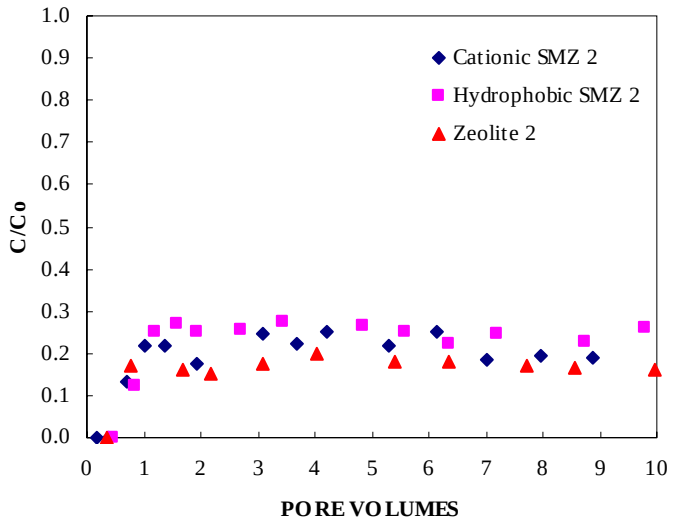

Appendix Figure D-9. **Observed microsphere BTCs for 5-µm microspheres (*Crypotosporidium*) of Cationic SMZ 2, Hydrophobic SMZ 2, and Zeolite 2.**

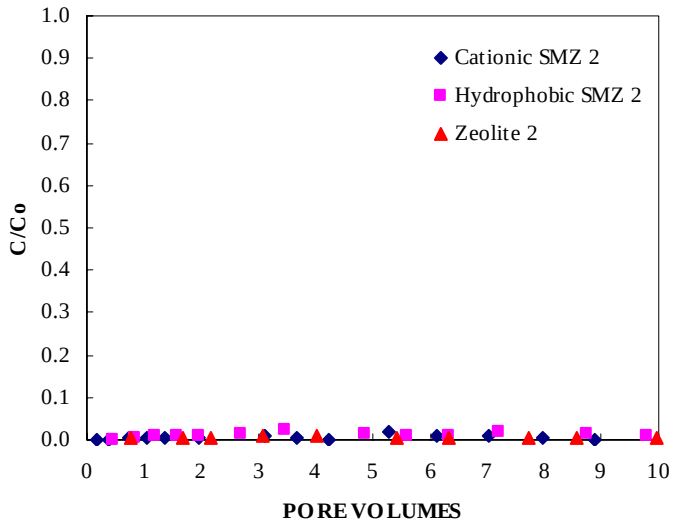

Appendix Figure D-10. **Observed microsphere BTCs for 10-µm microspheres (*Giardia*) of Cationic SMZ 2, Hydrophobic SMZ 2, and Zeolite 2.**

Appendix Table D-4. Microsphere BTC data.

Cationic SMZ 1			Cationic SMZ 2			Hydrophobic SMZ 1			Hydrophobic SMZ 2			Zeolite 1			Zeolite 2		
PV	5 µm C/Co	10 µm C/Co	PV	5 µm C/Co	10 µm C/Co	PV	5 µm C/Co	10 µm C/Co	PV	5 µm C/Co	10 µm C/Co	PV	5 µm C/Co	10 µm C/Co	PV	5 µm C/Co	10 µm C/Co
0.16	0.00	0.00	0.16	0.00	0.00	0.16	0.00	0.00	0.19	0.00	0.00	0.38	0.00	0.00	0.08	-	0.00
0.37	0.00	0.00	0.40	0.00	0.00	0.38	0.00	0.00	0.46	0.00	0.00	0.80	0.19	0.01	0.37	0.00	-
0.65	0.08	0.00	0.72	0.13	0.01	0.67	0.05	0.00	0.83	0.12	0.00	1.23	0.19	0.01	0.76	0.17	0.00
0.91	0.20	0.01	1.03	0.22	0.01	0.95	0.21	0.01	1.20	0.25	0.01	1.67	0.17	0.01	1.69	0.16	0.01
1.17	0.21	0.01	1.35	0.22	0.01	1.23	0.22	0.01	1.57	0.27	0.01	2.10	0.19	0.01	2.16	0.15	0.01
2.19	0.21	0.00	1.94	0.18	0.01	2.32	0.19	0.00	1.95	0.25	0.01	2.97	0.19	0.01	3.09	0.17	0.01
2.70	0.25	0.01	3.10	0.25	0.01	2.81	0.18	0.00	2.70	0.26	0.01	4.14	0.19	0.01	4.03	0.20	0.01
3.76	0.21	0.01	3.67	0.22	0.01	3.85	0.24	0.02	3.45	0.27	0.02	5.39	0.19	0.01	5.42	0.18	0.01
4.27	0.19	0.00	4.22	0.25	0.00	4.90	0.23	0.00	4.86	0.27	0.01	6.21	0.20	0.01	6.34	0.18	0.00
5.52	0.16	0.04	5.28	0.22	0.02	5.67	0.18	0.00	5.60	0.25	0.01	7.00	0.15	0.00	7.72	0.17	0.01
6.21	0.19	0.01	6.12	0.25	0.01	7.19	0.18	0.01	6.34	0.22	0.01	8.17	0.19	0.01	8.57	0.16	0.00
6.94	0.21	0.00	7.02	0.18	0.01	8.69	0.23	0.01	7.20	0.25	0.02	9.80	0.19	0.01	9.97	0.16	0.00
7.63	0.15	0.00	7.97	0.19	0.01	9.53	0.26	0.00	8.75	0.23	0.01	10.23	0.16	0.01	10.63	0.17	0.01
8.27	0.17	0.01	8.89	0.19	0.00	10.44	0.33	0.01	9.80	0.26	0.01						
8.92	0.17	0.00	10.88	0.21	0.01				10.92	0.18	0.01						
									12.04	0.13	0.01						
									13.21	0.21	0.01						

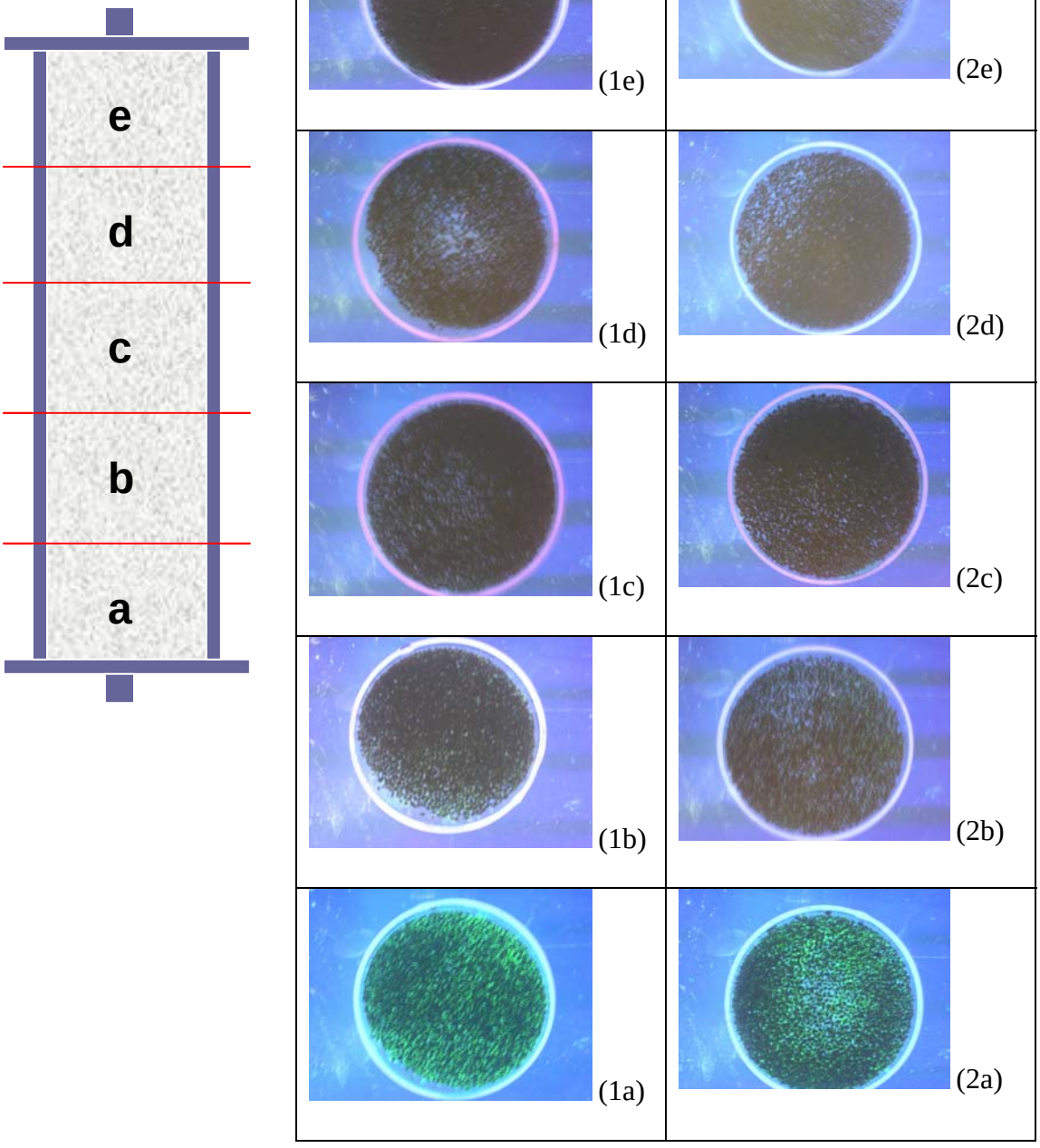

Appendix Figure D-11. **Visual inspection of fluorescent microspheres under ultraviolet light, Zeolite 1 (1a)-(1e) and Zeolite 2 (2a)-(2e) columns. Sections (a) through (e) corresponding to those taken from the bottom (1a) and (2a), near the inlet, up the column length.**

APPENDIX E. ELECTROPHORETIC MOBILITY DATA SHEETS

Presented are the electrophoretic mobility data sheets that were obtained from the DELSA 440SX to test the zeta potentials of the 5- and 10-μm microspheres, cationic SMZ, hydrophobic SMZ, and zeolite particles, which were described in the manuscript. The DELSA 440SX utilizes laser light, four photodiodes and four 256-channel autocorrelators to discriminate between particles from four optimized angles to detect very small zeta potential differences. One to four angles measurements were obtained for each run which are shown as peaks in the following plots. The average of these peaks is the zeta potential corresponding to the top (upper) or bottom (low) the flow cell. For each sample, the top and bottom values of the flow cell was measured and the average of the two was reported as the zeta potential measurement for the material. Lazer Zee calibration data sheets for the DELSA 440SX are also presented in this appendix.

Filename	012304.006		
Group ID	012304		
Sample ID	10u, up layer		
Operator	Charlotte		
Temperature	25.2 C	Set Temperature	25.2 C
Conductivity	0.177 mS/cm	Viscosity	0.0089 poise
Refractive Index	1.333	Dielectric Const.	78.36
Cell Constant	20.3889 1/cm	Cell Position	16
Frequency Range	1000 Hz	Frequency Shift	500 Hz
Current	0.2 mA	Cell Field	35.1 V/cm
On Time	2.5 s	Off Time	0.5 s
Start Time	15:05 23 Jan 2004	Elapsed Time	94 s

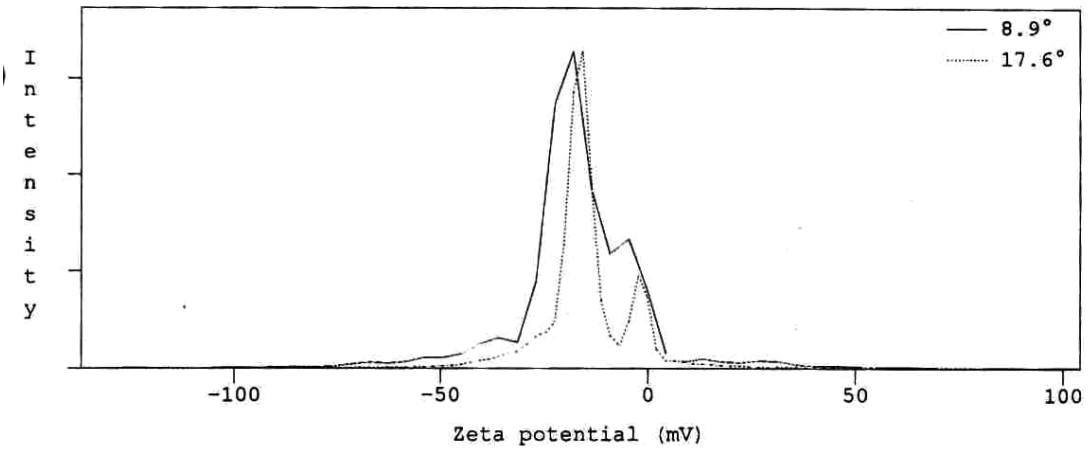

Peak Moment Analysis 012304.006 Zeta potential (mV)

-137 to 103 mV

Peak #1	Mode	Mean	S.D.	Skew
8.9°	-18	-16.5	16.6	10.8
17.6°	-15.7	-14.6	13.5	-7.45
Avg	-16.8	-15.5	15.1	1.65

Filename	012304.007		
Group ID	012304		
Sample ID	10u, low layer		
Operator	Charlotte		
Temperature	25.2 C	Set Temperature	25.2 C
Conductivity	0.177 mS/cm	Viscosity	0.0089 poise
Refractive Index	1.333	Dielectric Const.	78.36
Cell Constant	20.3889 1/cm	Cell Position	16
Frequency Range	1000 Hz	Frequency Shift	500 Hz
Current	0.2 mA	Cell Field	35.1 V/cm
On Time	2.5 s	Off Time	0.5 s
Start Time	15:07 23 Jan 2004	Elapsed Time	92 s

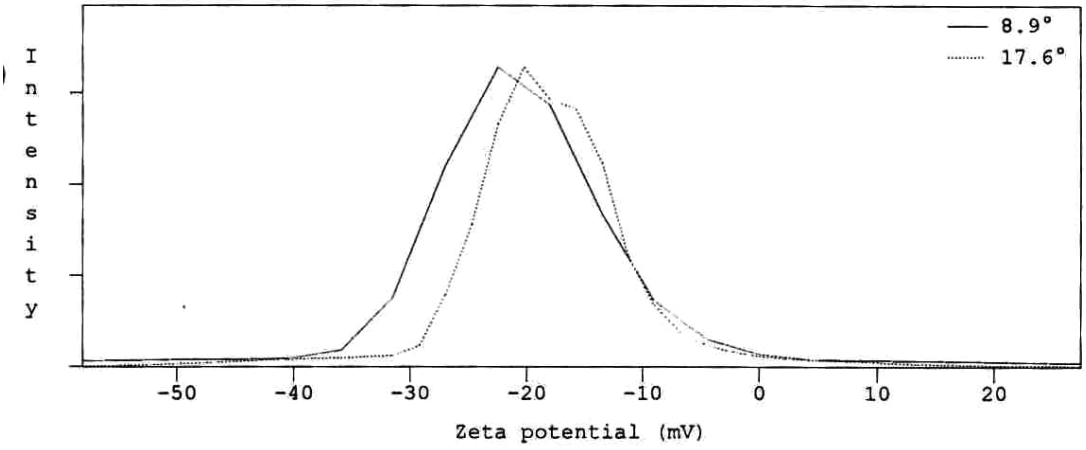

Peak Moment Analysis 012304.007 Zeta potential (mV)

-58.1 to 27.1 mV

Peak #1	Mode	Mean	S.D.	Skew
8.9°	-22.5	-20	9.69	9.13
17.6°	-20.2	-18	7.57	4.6
Avg	-21.3	-19	8.63	6.87

COULTER

DELSA 440SX 2.03

23 Jan 2004

Filename	012304.002		
Group ID	012304		
Sample ID	Laser Zee, up layer		
Operator	Charlotte		
Temperature	25.1 C	Set Temperature	25.1 C
Conductivity	0.862 mS/cm	Viscosity	0.0089 poise
Refractive Index	1.333	Dielectric Const.	78.36
Cell Constant	20.3889 1/cm	Cell Position	16
Frequency Range	1000 Hz	Frequency Shift	500 Hz
Current	0.7 mA	Cell Field	25.2 V/cm
On Time	2.5 s	Off Time	0.5 s
Start Time	14:23 23 Jan 2004	Elapsed Time	94 s

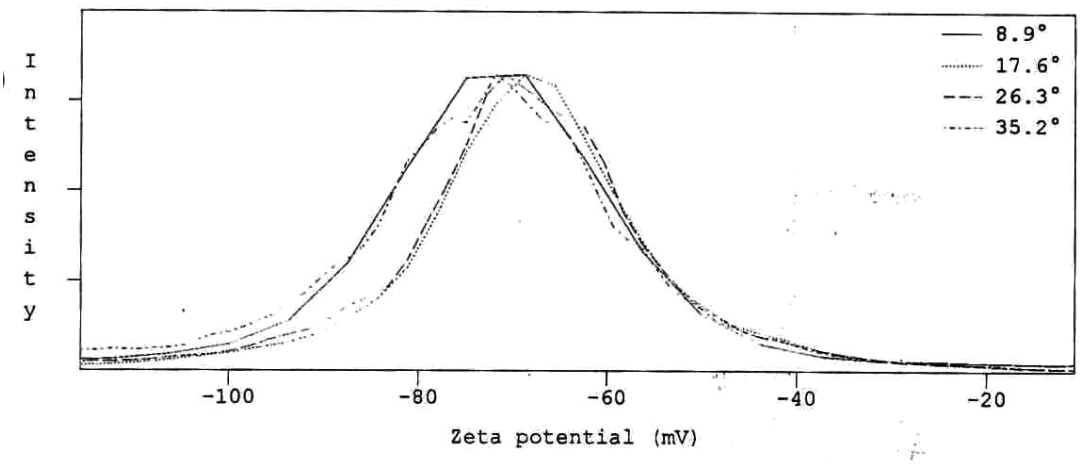

Peak Moment Analysis 012304.002 Zeta potential (mV)

-116 to -11.2 mV

Peak #1	Mode	Mean	S.D.	Skew
8.9°	-68.7	-70.6	15.2	12.4
17.6°	-68.7	-67.6	14.5	7.98
26.3°	-70.8	-68.2	14.7	7.63
35.2°	-71.8	-71.7	16	9.17
Avg	-70	-69.5	15.1	9.29

Filename	012304.002		
Group ID	012304		
Sample ID	Laser Zee, up layer		
Operator	Charlotte		
Temperature	25.1 C	Set Temperature	25.1 C
Conductivity	0.862 mS/cm	Viscosity	0.0089 poise
Refractive Index	1.333	Dielectric Const.	78.36
Cell Constant	20.3889 1/cm	Cell Position	16
Frequency Range	1000 Hz	Frequency Shift	500 Hz
Current	0.7 mA	Cell Field	25.2 V/cm
On Time	2.5 s	Off Time	0.5 s
Start Time	14:23 23 Jan 2004	Elapsed Time	94 s

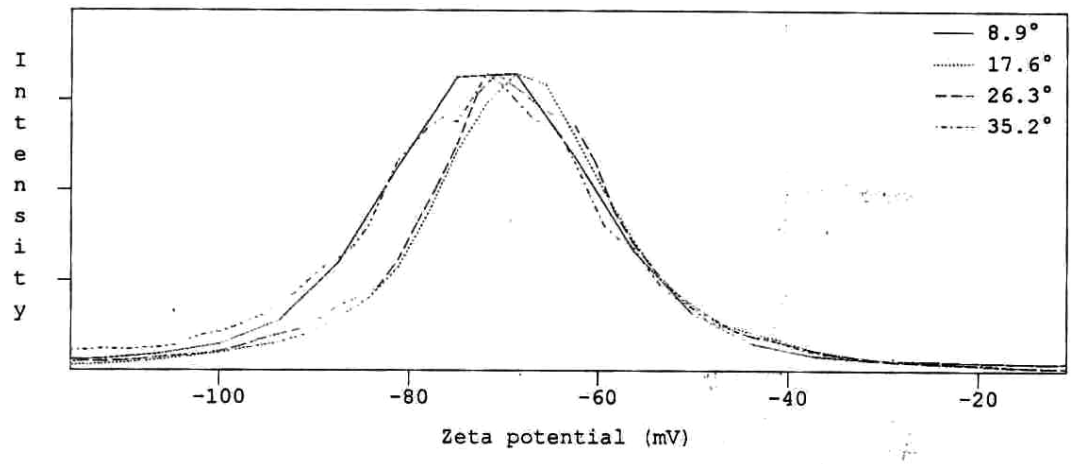

Peak Moment Analysis 012304.002 Zeta potential (mV)

-116 to -11.2 mV

Peak #1	Mode	Mean	S.D.	Skew
8.9°	-68.7	-70.6	15.2	12.4
17.6°	-68.7	-67.6	14.5	7.98
26.3°	-70.8	-68.2	14.7	7.63
35.2°	-71.8	-71.7	16	9.17
Avg	-70	-69.5	15.1	9.29

DELSA 440SX 2.03

COULTER

27 Feb 2004

Filename	270204.004		
Group ID	270204		
Sample ID	5 um bead , up layer		
Temperature	25.0 C	Set Temperature	25.0 C
Conductivity	0.24 mS/cm	Viscosity	0.0089 poise
Refractive Index	1.333	Dielectric Const.	78.36
Cell Constant	20.3052 1/cm	Cell Position	16
Frequency Range	1000 Hz	Frequency Shift	500 Hz
Current	0.15 mA	Cell Field	19.4 V/cm
On Time	2.5 s	Off Time	0.5 s
Start Time	15:28 27 Feb 2004	Elapsed Time	92 s

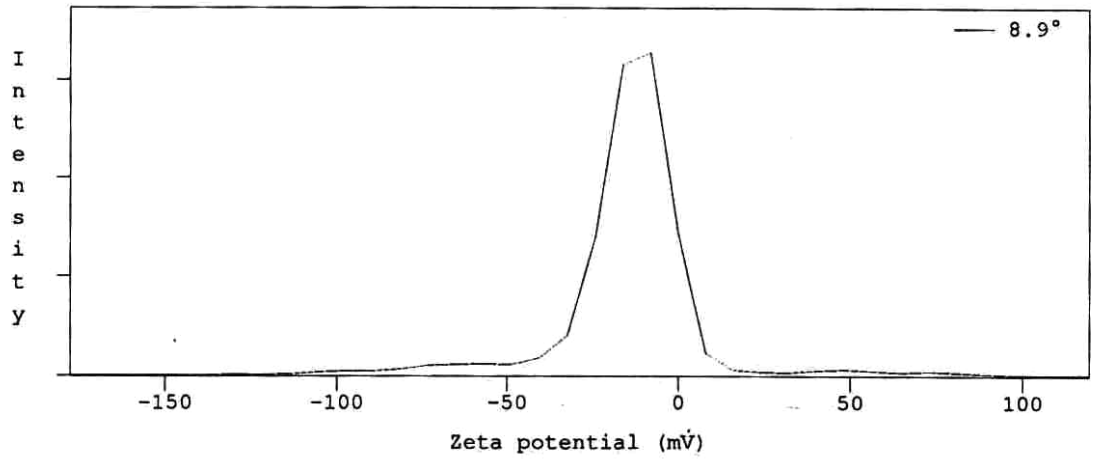

Peak Moment Analysis 270204.004 Zeta potential (mV)

-178 to 118 mV

Peak #1	Mode	Mean	S.D.	Skew
8.9°	-8.11	-14.4	21.4	-17.6
Avg	-8.11	-14.4	21.4	-17.6

DELSA 440SX 2.03

COULTER

27 Feb 2004

Filename	270204.003		
Group ID	270204		
Sample ID	5 um bead , low layer		
Temperature	25.2 C	Set Temperature	25.2 C
Conductivity	0.243 mS/cm	Viscosity	0.0089 poise
Refractive Index	1.333	Dielectric Const.	78.36
Cell Constant	20.3052 1/cm	Cell Position	16
Frequency Range	1000 Hz	Frequency Shift	500 Hz
Current	0.2 mA	Cell Field	25.6 V/cm
On Time	2.5 s	Off Time	0.5 s
Start Time	15:22 27 Feb 2004	Elapsed Time	95 s

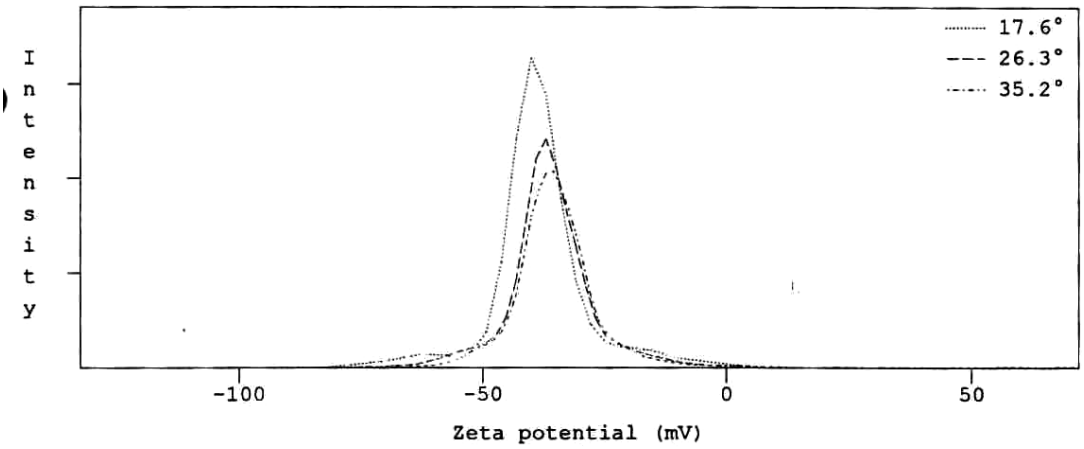

Peak Moment Analysis 270204.003 Zeta potential (mV)

-133 to 71 mV

Peak #1	Mode	Mean	S.D.	Skew
17.6°	-40	-38	11.6	12.2
26.3°	-37	-35.2	12.7	17.6
35.2°	-196	-33.7	13.3	19.4
Avg	-90.9	-35.6	12.5	16.4

Filename	270204.001		
Group ID	270204		
Sample ID	Laser Zee Std, up layer		
Comment	Settings for Coulter mobility control		
Temperature	25.0 C	Set Temperature	25.0 C
Conductivity	0.865 mS/cm	Viscosity	0.0089 poise
Refractive Index	1.333	Dielectric Const.	78.36
Cell Constant	20.3052 1/cm	Cell Position	16
Frequency Range	1000 Hz	Frequency Shift	500 Hz
Current	0.7 mA	Cell Field	25.1 V/cm
On Time	2.5 s	Off Time	0.5 s
Start Time	15:09 27 Feb 2004	Elapsed Time	94 s

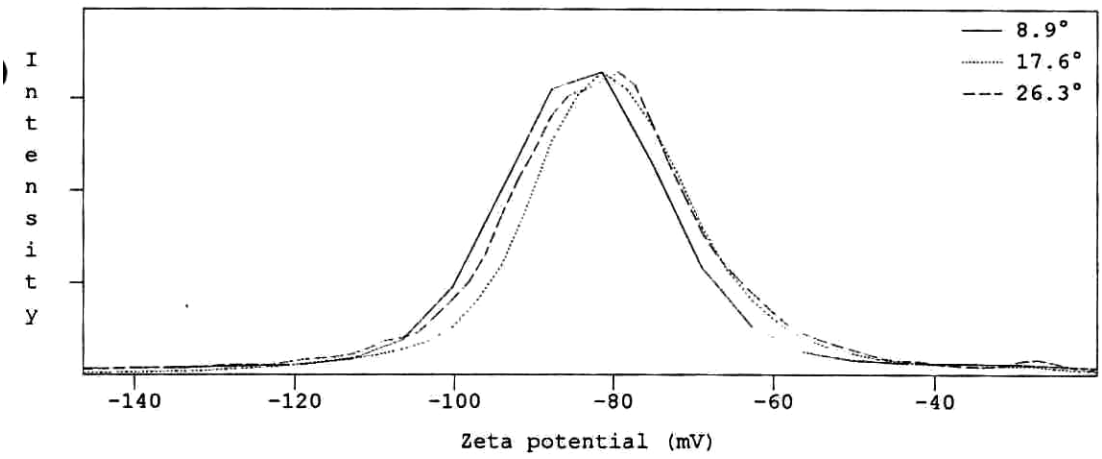

Peak Moment Analysis 270204.001 Zeta potential (mV)

-147 to -20.3 mV

Peak #1	Mode	Mean	S.D.	Skew
8.9°	-81.5	-83.3	16.2	7.81
17.6°	-81.5	-79.9	15.3	6.96
26.3°	-79.4	-81.3	17	-3.85
Avg	-80.8	-81.5	16.2	3.64

Filename	270204.002		
Group ID	270204		
Sample ID	Laser Zee Std, low layer		
Comment	Settings for Coulter mobility control		
Temperature	25.0 C	Set Temperature	25.0 C
Conductivity	0.865 mS/cm	Viscosity	0.0089 poise
Refractive Index	1.333	Dielectric Const.	78.36
Cell Constant	20.3052 1/cm	Cell Position	16
Frequency Range	1000 Hz	Frequency Shift	500 Hz
Current	0.7 mA	Cell Field	25.1 V/cm
On Time	2.5 s	Off Time	0.5 s
Start Time	15:12 27 Feb 2004	Elapsed Time	93 s

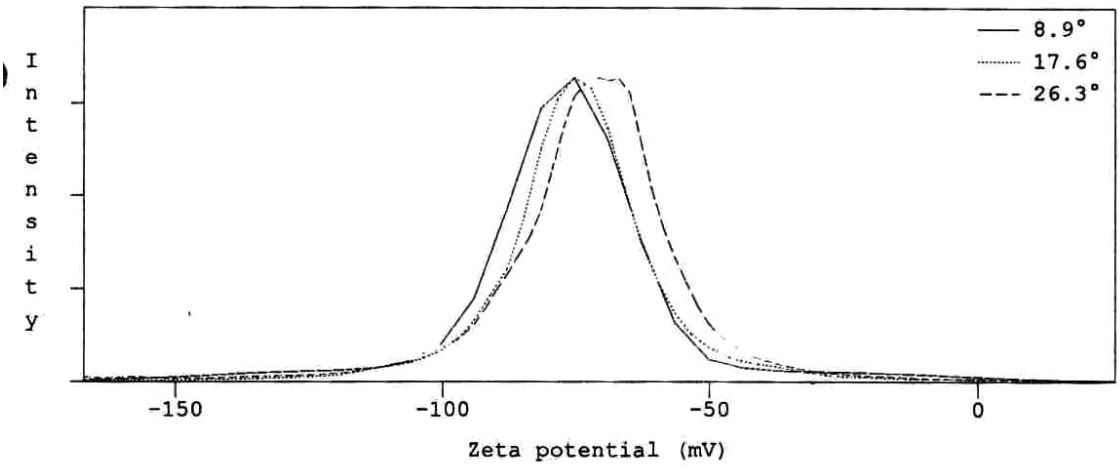

Peak Moment Analysis 270204.002 Zeta potential (mV)

-167 to 24.8 mV

Peak #1	Mode	Mean	S.D.	Skew
8.9°	-75.2	-76.5	19.9	9.32
17.6°	-75.2	-74.4	16.4	8.13
26.3°	-71	-72.4	18.7	-17
Avg	-73.8	-74.4	18.4	0.142

Filename	.001		
Group ID			
Sample ID			
Temperature	25.1 C	Set Temperature	25.1 C
Conductivity	0.865 mS/cm	Viscosity	0.0089 poise
Refractive Index	1.333	Dielectric Const.	78.36
Cell Constant	20.3171 1/cm	Cell Position	16
Frequency Range	1000 Hz	Frequency Shift	500 Hz
Current	0.7 mA	Cell Field	25.1 V/cm
On Time	2.5 s	Off Time	0.5 s
Start Time	14:30 29 Jan 2004	Elapsed Time	92 s

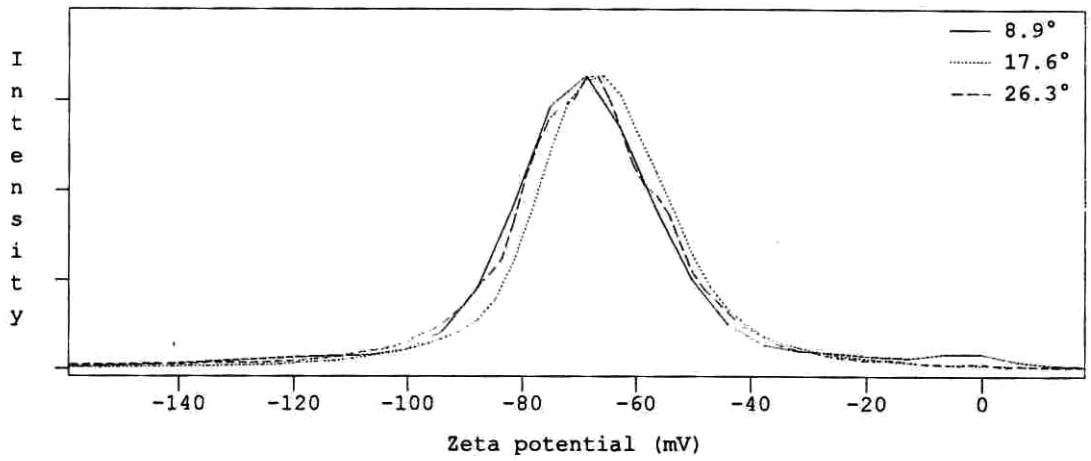

Peak Moment Analysis .001 Zeta potential (mV)

-159 to 17.2 mV

Peak #1	Mode	Mean	S.D.	Skew
8.9°	-68.9	-67.8	21.5	12.5
17.6°	-65.8	-65.6	17.8	-6.68
26.3°	-66.8	-68.8	19.7	-14.7
Avg	-67.2	-67.4	19.7	-2.95

DELSA 440SX 2.03

COULTER

29 Jan 2004

Filename	.001		
Group ID			
Sample ID			
Temperature	25.1 C	Set Temperature	25.1 C
Conductivity	0.865 mS/cm	Viscosity	0.0089 poise
Refractive Index	1.333	Dielectric Const.	78.36
Cell Constant	20.3171 1/cm	Cell Position	16
Frequency Range	1000 Hz	Frequency Shift	500 Hz
Current	0.7 mA	Cell Field	25.1 V/cm
On Time	2.5 s	Off Time	0.5 s
Start Time	14:30 29 Jan 2004	Elapsed Time	92 s

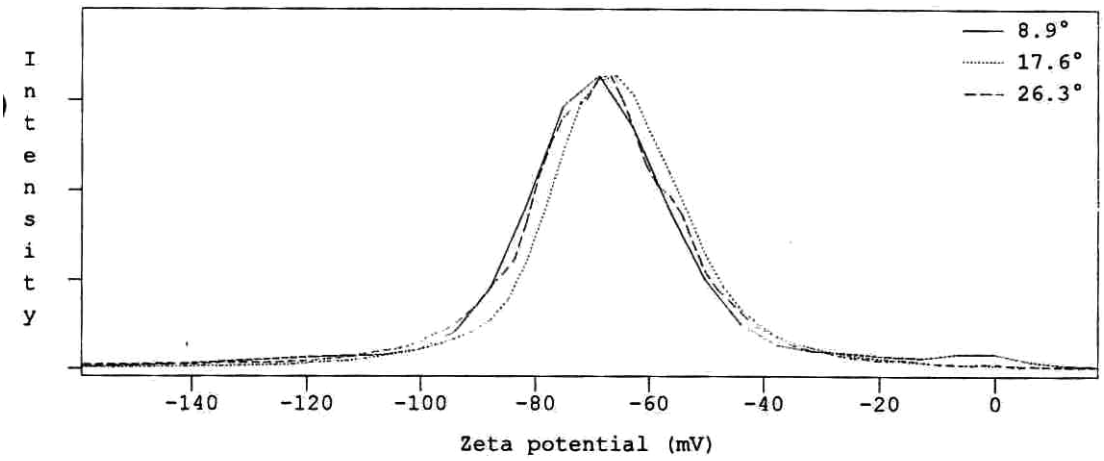

Peak Moment Analysis .001 Zeta potential (mV)

-159 to 17.2 mV

Peak #1	Mode	Mean	S.D.	Skew
8.9°	-68.9	-67.8	21.5	12.5
17.6°	-65.8	-65.6	17.8	-6.68
26.3°	-66.8	-68.8	19.7	-14.7
Avg	-67.2	-67.4	19.7	-2.95

COULTER

DELSA 440SX 2.03

29 Jan 2004

Filename	012904.005		
Group ID	012904		
Sample ID	CationicSMZ1, up layer		
Operator	Charlotte		
Temperature	25.1 C	Set Temperature	25.1 C
Conductivity	0.298 mS/cm	Viscosity	0.0089 poise
pH	7.39		
Refractive Index	1.333	Dielectric Const.	78.36
Cell Constant	20.3171 1/cm	Cell Position	16
Frequency Range	1000 Hz	Frequency Shift	500 Hz
Current	0.15 mA	Cell Field	15.6 V/cm
On Time	2.5 s	Off Time	0.5 s
Start Time	15:32 29 Jan 2004	Elapsed Time	94 s

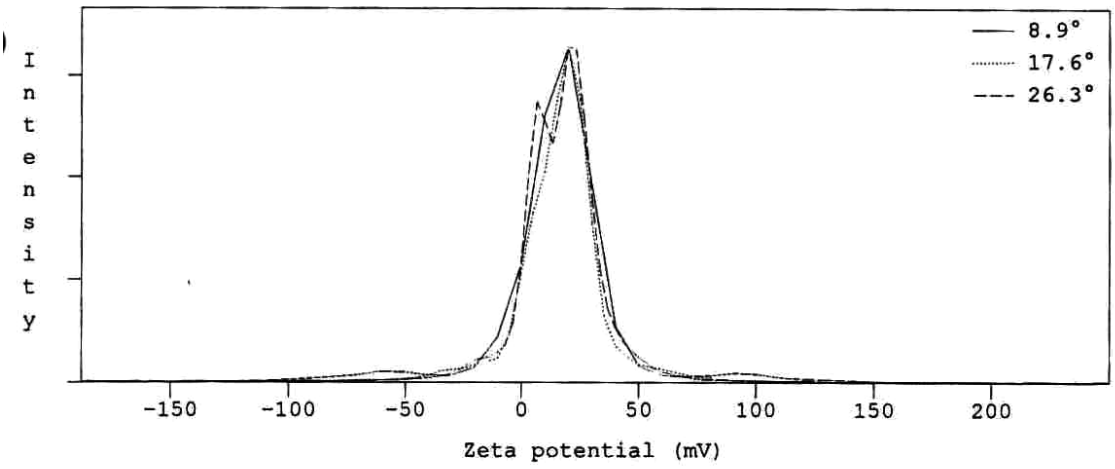

Peak Moment Analysis 012904.005 Zeta potential (mV)

-185 to 241 mV

Peak #1	Mode	Mean	S.D.	Skew
8.9°	20.1	16.5	27.5	-12.7
17.6°	20.1	17.2	19.8	14.8
26.3°	20.1	17.1	21.5	15.4
Avg	20.1	16.9	22.9	5.82

Filename	012904.006		
Group ID	012904		
Sample ID	CationicSMZ1, low layer		
Operator	Charlotte		
Temperature	25.1 C	Set Temperature	25.1 C
Conductivity	0.297 mS/cm	Viscosity	0.0089 poise
pH	7.39		
Refractive Index	1.333	Dielectric Const.	78.36
Cell Constant	20.3171 1/cm	Cell Position	16
Frequency Range	1000 Hz	Frequency Shift	500 Hz
Current	0.15 mA	Cell Field	15.7 V/cm
On Time	2.5 s	Off Time	0.5 s
Start Time	15:36 29 Jan 2004	Elapsed Time	92 s

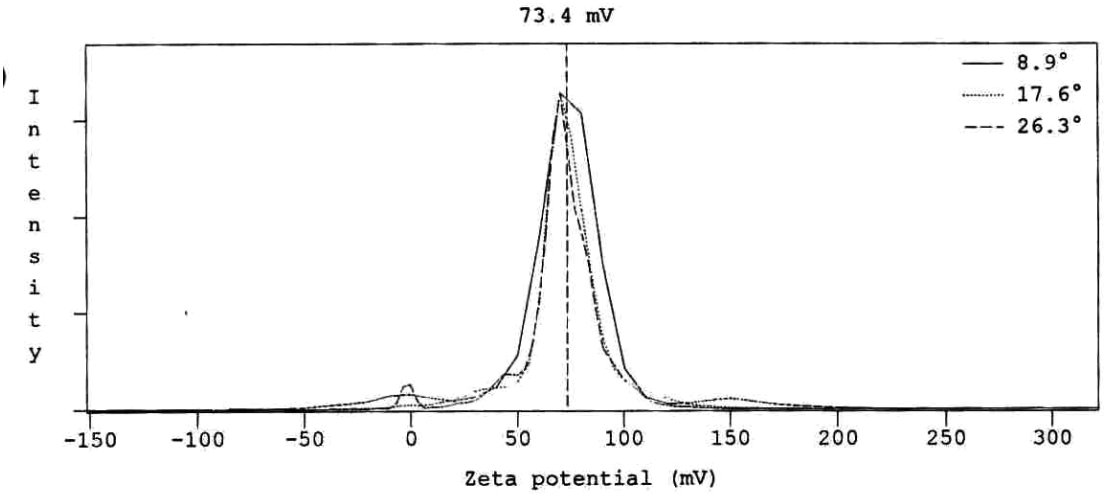

Peak Moment Analysis 012904.006 Zeta potential (mV)

-152 to 320 mV

Peak #1	Mode	Mean	S.D.	Skew
8.9°	70.3	72.3	29.5	-22.3
17.6°	70.3	72.9	19.4	-15.4
26.3°	70.3	72.5	21.3	14
Avg	70.3	72.6	23.4	-7.93

DELSA 440SX 2.03

COULTER

29 Jan 2004

Filename	012904.008		
Group ID	012904		
Sample ID	hydrophobicSMZ1, up layer		
Operator	Charlotte		
Temperature	25.1 C	Set Temperature	25.1 C
Conductivity	0.243 mS/cm	Viscosity	0.0089 poise
pH	7.39		
Refractive Index	1.333	Dielectric Const.	78.36
Cell Constant	20.3171 1/cm	Cell Position	16
Frequency Range	1000 Hz	Frequency Shift	500 Hz
Current	0.15 mA	Cell Field	19.2 V/cm
On Time	2.5 s	Off Time	0.5 s
Start Time	15:59 29 Jan 2004	Elapsed Time	93 s

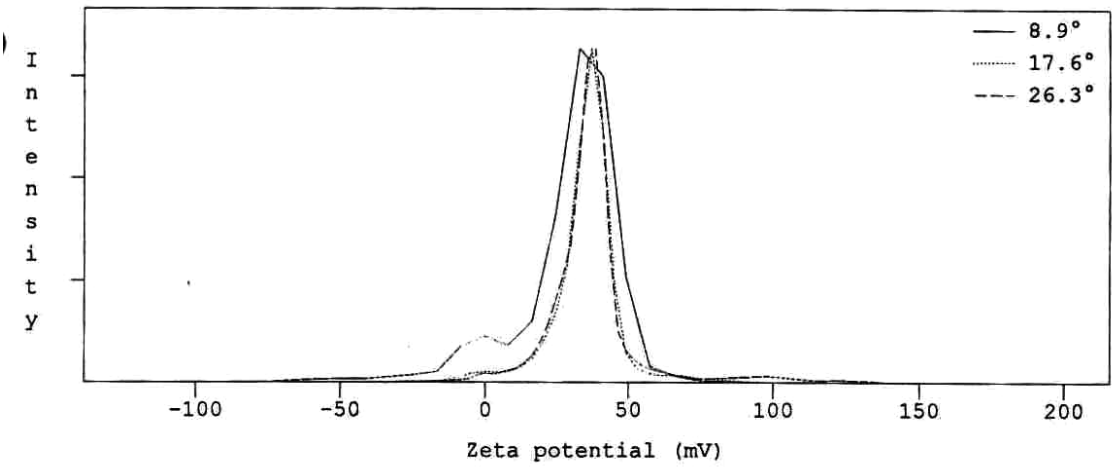

Peak Moment Analysis 012904.008 Zeta potential (mV)

-139 to 214 mV

Peak #1	Mode	Mean	S.D.	Skew
8.9°	32.9	31.2	23.2	-16.9
17.6°	37	34.9	15.6	-11.2
26.3°	38.3	34.9	13.9	-11.2
Avg	36.1	33.7	17.6	-13.1

COULTER

DELSA 440SX 2.03

29 Jan 2004

Filename	012904.007		
Group ID	012904		
Sample ID	hydrophobicSMZ1, low layer		
Operator	Charlotte		
Temperature	25.3 C	Set Temperature	25.3 C
Conductivity	0.244 mS/cm	Viscosity	0.0089 poise
pH	7.39		
Refractive Index	1.333	Dielectric Const.	78.36
Cell Constant	20.3171 1/cm	Cell Position	16
Frequency Range	1000 Hz	Frequency Shift	500 Hz
Current	0.15 mA	Cell Field	19.1 V/cm
On Time	2.5 s	Off Time	0.5 s
Start Time	15:56 29 Jan 2004	Elapsed Time	93 s

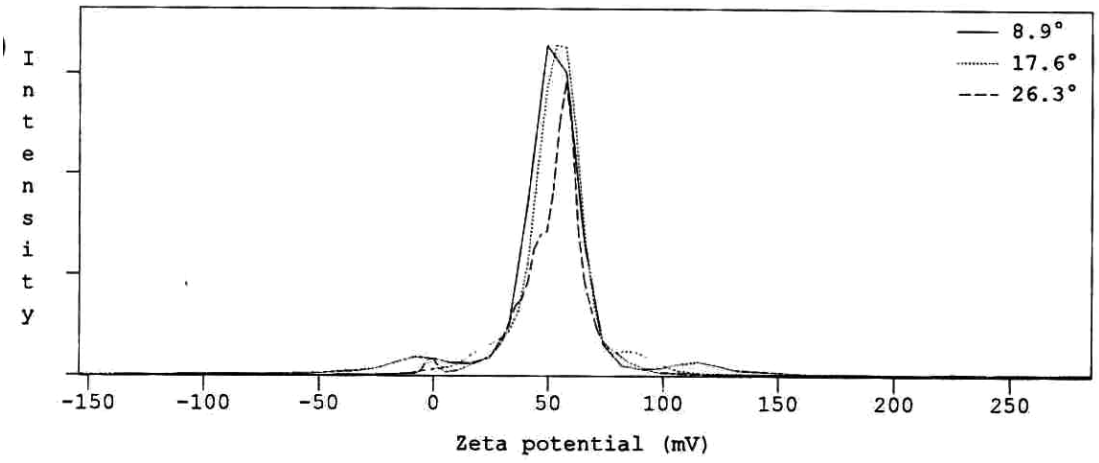

Peak Moment Analysis 012904.007 Zeta potential (mV)

-154 to 284 mV

Peak #1	Mode	Mean	S.D.	Skew
8.9°	49.5	51.1	24.6	-16.8
17.6°	53.6	54.7	16.1	9.59
26.3°	57.7	56.4	19.8	27.9
Avg	53.6	54	20.2	6.9

COULTER

DELSA 440SX 2.03

29 Jan 2004

Filename	012904.003		
Group ID	012904		
Sample ID	Zeolite1, up layer		
Operator	Charlotte		
Temperature	25.0 C	Set Temperature	25.0 C
Conductivity	0.204 mS/cm	Viscosity	0.0089 poise
pH	7.39		
Refractive Index	1.333	Dielectric Const.	78.36
Cell Constant	20.3171 1/cm	Cell Position	16
Frequency Range	1000 Hz	Frequency Shift	500 Hz
Current	0.2 mA	Cell Field	30.4 V/cm
On Time	2.5 s	Off Time	0.5 s
Start Time	14:57 29 Jan 2004	Elapsed Time	90 s

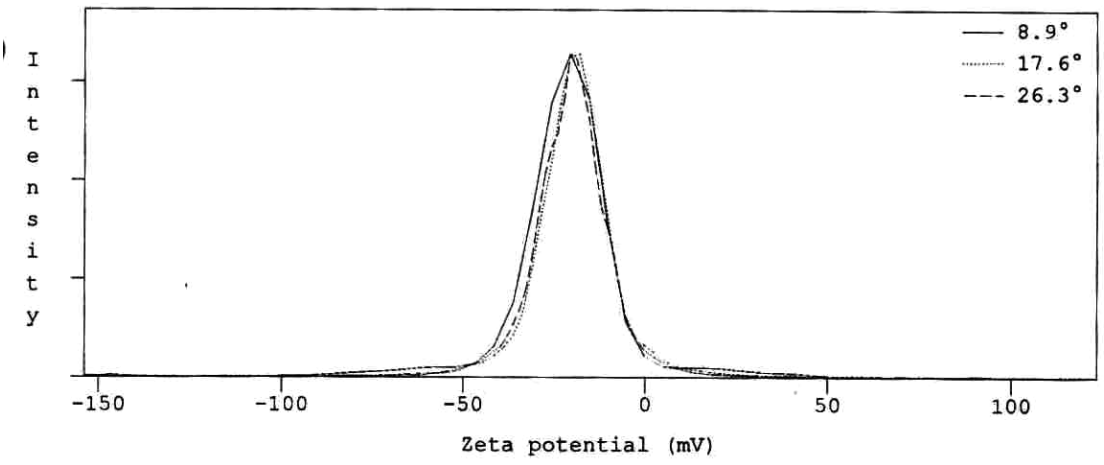

Peak Moment Analysis 012904.003 Zeta potential (mV)

-154 to 122 mV

Peak #1	Mode	Mean	S.D.	Skew
8.9°	-20.7	-21.1	16.2	12.6
17.6°	-18.1	-19.1	16.4	13.7
26.3°	-20.7	-20.4	12.8	-15.9
Avg	-19.8	-20.2	15.1	3.45

DELSA 440SX 2.03

COULTER

29 Jan 2004

Filename	012904.002		
Group ID	012904		
Sample ID	Zeolitel, low layer		
Operator	Charlotte		
Temperature	25.1 C	Set Temperature	25.1 C
Conductivity	0.204 mS/cm	Viscosity	0.0089 poise
pH	7.39		
Refractive Index	1.333	Dielectric Const.	78.36
Cell Constant	20.3171 1/cm	Cell Position	16
Frequency Range	1000 Hz	Frequency Shift	500 Hz
Current	0.2 mA	Cell Field	30.4 V/cm
On Time	2.5 s	Off Time	0.5 s
Start Time	14:54 29 Jan 2004	Elapsed Time	92 s

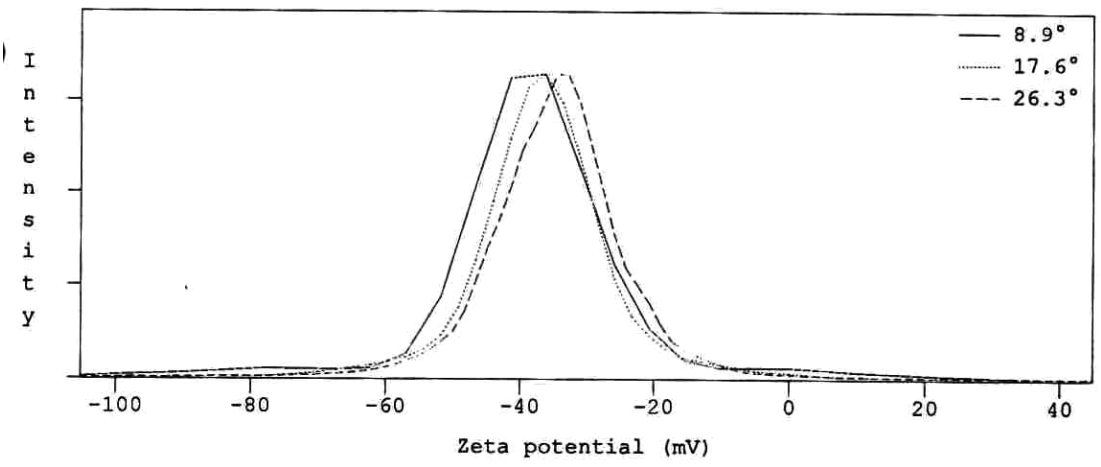

Peak Moment Analysis 012904.002 Zeta potential (mV)

-105 to 44.2 mV

Peak #1	Mode	Mean	S.D.	Skew
8.9°	-36.2	-37.6	14.8	8.2
17.6°	-36.2	-36.2	11.7	9.79
26.3°	-34.5	-34.3	11.5	8.03
Avg	-35.6	-36	12.7	8.67